ALMA MATER STUDIORUM
UNIVERSITÀ DI BOLOGNA

ARCHIVIO ISTITUZIONALE
DELLA RICERCA

Alma Mater Studiorum Università di Bologna
Archivio istituzionale della ricerca

Economic and environmental benefits by improved process control strategies in HCl removal from waste-to-energy flue gas

This is the final peer-reviewed author's accepted manuscript (postprint) of the following publication:

Published Version:
Dal Pozzo A., Muratori G., Antonioni G., Cozzani V. (2021). Economic and environmental benefits by improved process control strategies in HCl removal from waste-to-energy flue gas. WASTE MANAGEMENT, 125, 303-315 [10.1016/j.wasman.2021.02.059].

Availability:
This version is available at: https://hdl.handle.net/11585/821276 since: 2021-05-31

Published:
DOI: http://doi.org/10.1016/j.wasman.2021.02.059

Terms of use:

Some rights reserved. The terms and conditions for the reuse of this version of the manuscript are specified in the publishing policy. For all terms of use and more information see the publisher's website.

This item was downloaded from IRIS Università di Bologna (https://cris.unibo.it/).
When citing, please refer to the published version.

(Article begins on next page)

16 September 2026

Economic and environmental benefits by improved process control strategies in HCl removal from waste-to-energy flue gas

HIGHLIGHTS

*Alessandro Dal Pozzo, Giacomo Muratori, Giacomo Antonioni, Valerio Cozzani**
LISES - Dipartimento di Ingegneria Civile, Chimica, Ambientale e dei Materiali, Alma Mater Studiorum - Università di Bologna, via Terracini n.28, 40131 Bologna, Italy

(*)*corresponding author*, Tel. +39-051-2090240, Fax +39-051-2090247, e-mail: valerio.cozzani@unibo.it

- A methodology was outlined to test control strategies in operating facilities
- A virtual console was used to reproduce system behaviour
- Environmental, Economic and Technical performance indicators were defined
- Improved control strategies result in higher Environmental and Economic performance
- Full-scale test-runs confirmed the effectiveness of alternative control strategies

Economic and environmental benefits by improved process control strategies in HCl removal from waste-to-energy flue gas

*Alessandro Dal Pozzo, Giacomo Muratori, Giacomo Antonioni, Valerio Cozzani**
LISES - Dipartimento di Ingegneria Civile, Chimica, Ambientale e dei Materiali, Alma Mater Studiorum - Università di Bologna, via Terracini n.28, 40131 Bologna, Italy

(*)*corresponding author*, Tel. +39-051-2090240, Fax +39-051-2090247, e-mail: valerio.cozzani@unibo.it

Abstract

The control of HCl emission in waste-to-energy (WtE) facilities is a challenging flue gas treatment problem: the release of HCl from waste combustion is highly variable in time and the HCl emission standards are typically far lower in WtE than in any other industry. Traditional process control approaches in dry HCl removal processes are generally based on feeding a large excess of solid reactants to the system, to ensure robustness and a wide safety margin in the compliance to environmental regulations. This results in the production of a high amount of unreacted sorbents, strongly increasing the generation of solid wastes that need to be disposed. In the present study, an approach was developed to allow the implementation of improved control strategies for dry HCl abatement systems in operating full-scale facilities. Its objective is the reduction of the reactant feed and the waste production, while still providing an adequate safety margin for emission compliance. The approach was based on the reproduction of the behaviour of the real system in a virtual console that allows the extensive testing of alternative control strategies, limiting the need of demanding test-runs at the real plant. A test case on an Italian WtE facility demonstrated the capability of a control logic tuned in the virtual console to achieve a 13% reduction in the consumption of reactants and generation of process residues, with unchanged HCl removal

efficiency. The results evidence the wide opportunities for optimisation of dry acid gas removal systems, in particular when multistage systems are implemented.

Keywords: waste-to-energy, HCl, process optimization, dry sorbent injection.

1 Introduction

In a modern waste management system, waste-to-energy (WtE) facilities have the role to divert from landfilling waste streams for which recycling is currently technically or economically unfeasible (Nizami et al., 2016) and enabling their thermal valorisation (Arena et al., 2015), thus facilitating the transition to a circular economy (Bagheri et al., 2020; Van Caneghem et al., 2019). Thanks to increasingly ambitious environmental regulations, the emission of several air pollutants related to WtE operation has been reduced more than tenfold in the last decades (Ardolino et al., 2020; Damgaard et al., 2010). However, in the current holistic approach to environmental protection, the reduction of impacts has to go beyond the minimisation of the emission of pollutants at the stack of the plant. Also indirect impacts, e.g. those associated to the consumption of reactants and the production of process residues in the flue gas treatment system of the plant (Dal Pozzo et al., 2017; Dong et al., 2020; Lausselet et al., 2016), needs to be minimised.

Hydrogen chloride (HCl) is a typical pollutant in WtE flue gases, arising from the combustion of waste containing chlorine (Zhang et al., 2019). Chlorine is widely dispersed amongst organic and inorganic compounds present in several waste items (Gerassimidou et al., 2020; Yang et al., 2018). Among the different techniques available for HCl removal (Bal et al., 2019; Dal Pozzo et al., 2019; Ephraim et al., 2019; Kameda et al., 2020), dry sorbent injection (DSI) is one of the technologies more frequently implemented (Beylot et al., 2018; Dal Pozzo et al., 2018a). DSI consists in the in-duct addition of an alkaline powdered reactant (e.g. calcium

hydroxide or sodium bicarbonate), which neutralises acid pollutants as HCl via gas-solid reaction (Antonioni et al., 2016). DSI, adopted in either single or two-stage configurations (Dal Pozzo et al., 2016; De Greef et al., 2013), is considered among the best available techniques for flue gas treatment in WtE installations recommended by the European Union (Neuwahl et al., 2019).

The main environmental drawback of DSI systems is the high stoichiometric excess of reactant feed that is required to achieve high HCl removal efficiency (Vehlow, 2015). The resulting excess consumption of reactant leads to the generation of relevant streams of solid process residues in the fabric filters, where they are collected together with fly ashes and micropollutants. The presence of these other components in the collected process residues causes the stream to be considered as hazardous waste and to require its disposal in dedicated landfill sites (Dal Pozzo et al., 2018b; Kameda et al., 2020).

In addition, given that the composition of the waste burnt in the combustion chamber of a WtE plant varies widely over time, the resulting extreme variability of HCl concentration at the inlet of the flue gas treatment section (Dal Pozzo et al., 2020) is an inherent instability that limits the effectiveness of conventional control strategies in calibrating the reactant feed needed to maintain a constant concentration setpoint at the outlet. Thus, the prevailing trend in control strategies is to calibrate the process control parameters of the DSI system on the safe side, and even more so accept high excess feed rates of reactants to minimise the possible occurrence of overruns of HCl emission limits at stack.

A more accurate setting of the DSI control system could ensure not only a safe compliance of emission limits at stack, but also a reduction of the consumption of reactants and the generation of process residues. These in principle represent an undesired environmental

74 burden shift between different compartments (from air to soil/water) (Bogush et al., 2015;
75 Margallo et al., 2015; Quina et al., 2018).
76 The problem of the optimisation of flue gas treatment control with reference either to the
77 WtE context or to acid pollutants (HCl, SO_2, HF) is scarcely addressed in scholarly literature.
78 Ting et al. (2008) described the design of a PID control for acid gas removal via semi-dry
79 scrubbing in a WtE plant, with parameter tuning performed during commissioning operation.
80 Gassner et al. (2014) explored the use of data-driven modelling approaches to describe the
81 non-stationary operational behaviour of a semi-dry flue gas desulfurization process. Cignitti
82 et al. (2016) developed a simple first principle model to predict the dynamics of a semidry SO_2
83 absorber in desulfurization units of coal-fired power plants, while Guo et al. (2019) used a
84 hybrid approach, blending first principles and neural network, to model and optimise a wet
85 flue gas desulfurization unit. Yet, the focus of these recent studies has been mainly the
86 theoretical development of enhanced dynamic models of the process, rather than their
87 implementation in real control schemes. In particular, to the best of the authors' knowledge,
88 no previous paper addresses the potential environmental and economic advantages in terms
89 of reduced reactant consumption and related waste generation achievable with process
90 control optimisation in WtE acid gas removal.
91 Furthermore, control optimisation in the WtE context is made complex by the fact that
92 conventional direct tuning via extensive test runs during plant operation is generally
93 incompatible with the need to comply with strict HCl emission limits in presence of a highly
94 variable inlet load of HCl coming from waste combustion. In this regard, the set-up of data-
95 driven simulations of the real system in a virtual environment, as more and more frequently
96 performed in the manufacturing (Goodall et al., 2019) and process industry (Kockmann,
97 2019), could drastically reduce the need of field tests. By this strategy, the screening and the

98 tuning of new control settings is carried out directly in a virtual set-up, thus limiting the
99 number of in-field test runs only to those needed for the initial calibration of the simulation
100 and for the final trial of the new control system.
101 The present study focuses on the development of an approach for the optimisation of process
102 control in a typical DSI system for HCl removal based on a virtual environment. A dynamic
103 simulation of the dry treatment system was built in a virtual console implemented using the
104 Simulink software. A data-driven process model, calibrated with a specific set of test data,
105 nested into a reproduction of the control system of the DSI unit, was thus obtained and
106 validated. The virtual console was used to test and tune an alternative control strategy, with
107 the objective to reduce the stoichiometric excess of reactant associated to HCl removal. The
108 alternative control was then tested in full scale at the real plant, demonstrating the potential
109 for significant environmental and economic benefits deriving from the reduction in reactant
110 consumption and related process waste generation.
111

2 Reference system and test facility

2.1 HCl removal system

The two-stage acid gas abatement system of a medium-sized (400 t/d of waste treated) WtE facility located in Northern Italy was used as case study. As shown in Fig. 1, this system is based on two consecutive steps of dry sorbent injection and filtration, taking place at ~180 °C, downstream of the heat recovery section of the plant. In the first stage, calcium hydroxide, $Ca(OH)_2$, is injected, triggering the following gas-solid reaction of HCl neutralisation (Iizuka et al., 2020):

$$Ca(OH)_2 + 2\,HCl \rightarrow CaCl_2 + 2\,H_2O \quad (1)$$

A fabric filter separates the solid product of reaction from the flue gas, together with a relevant unreacted fraction of $Ca(OH)_2$, present both due to the excess feed of reactant and for the intrinsic diffusional limitations of gas-solid reaction (i.e. the phenomenon of incomplete conversion discussed by Antonioni et al., 2016). In the second stage, the dry injection is based on sodium bicarbonate, $NaHCO_3$. At the injection temperature and, in general, at T > 130 °C (see Hartman et al., 2013), $NaHCO_3$ decomposes to porous sodium carbonate (Na_2CO_3), which in turn absorbs HCl (Dal Pozzo et al., 2019):

$$2\,NaHCO_3 \rightarrow Na_2CO_3 + CO_2 + H_2O \quad (2)$$

$$Na_2CO_3 + 2\,HCl \rightarrow 2\,NaCl + CO_2 + H_2O \quad (3)$$

Again, the solid product of reaction and an unreacted fraction of reactant are collected by a fabric filter. This two-stage configuration is adopted in several European WtE installations and it is appreciated for its built-in redundancy in terms of emission control (De Greef et al., 2013) and its flexibility that allows different repartitions of abatement demand between the two stages (Dal Pozzo et al., 2016).

As shown in Fig. 1, the present study is focused on the optimisation of the control of the $Ca(OH)_2$ 1st stage of acid gas removal, referred to in the following as dry sorbent injection (DSI) system. As discussed in the following, the optimisation and tuning of the process control of the 1st stage not only improves the performance of the stage, but, stabilising the HCl outlet concentration, it also favours the optimal performance of the 2nd stage.

2.2 Process control

In the test facility, a conventional process control scheme implemented in several similar plants is present. The operation of the two-stage acid gas abatement system is monitored by the continuous acquisition of flue gas composition data at the measurement points PM1, PM2 and EM indicated in Fig. 1. The concentration of the main gas species at the sampling points, including the acid pollutants (HCl, SO_2, HF), is measured by Fourier-Transform infrared (FTIR) spectrometry, in compliance with CEN/TS 17337 (CEN, 2019), while the flue gas flowrate is determined at stack (point EM) by means of S-type Pitot tube velocity measurements.

In both the acid gas abatement stages, the distributed control system (DCS) of the plant controls the solid reactant feed based on the measured inlet and outlet mass flowrates of acid pollutants. A conditional logic selects the reactant feed rate as the maximum of two values, calculated as follows:

i. *Feedforward criterion*. The calculated feed rate is equal to the stoichiometric demand related to the abatement of the inlet mass flowrates of acid pollutants at PM1, increased by a 10% excess.

ii. *Feedback criterion.* The feed rate is calculated according to a Proportional Integral (PI) feedback formula based on the difference between a set-point for the outlet HCl concentration and the value measured at PM2.

160 The settings of the feedback control (proportional gain K_P = 5 and integral gain τ_I = 8 s)
161 provide an aggressive reaction, i.e. strong excess feed rates of reactant are delivered
162 whenever the outlet HCl concentration exceeds the setpoint. Conversely, when the outlet HCl
163 concentration is lower than the setpoint, the feed rate of reactant does not drop as
164 significantly, because the feedforward criterion takes over. Thus, the combination of the
165 feedforward and feedback criteria as detailed above realises an asymmetrical control action,
166 in which the setpoint is actually treated as a threshold. The feedforward PI control works
167 merely as an environmental safeguard, intended to act only if the feedforward is not capable
168 to maintain the outlet below the given threshold. A survey carried out by the authors involving
169 several Italian companies (HERAmbiente, HestAmbiente, IREN, Brianza Energia Ambiente)
170 evidenced that this control strategy is typical of WtE acid gas abatement units, as the
171 objective is to avoid any spike in outlet HCl resulting from a variation in the inlet HCl load
172 coming from waste combustion (Muratori et al., 2020).
173
174 **2.3 Drawbacks of the reference control system**
175 The typical behaviour of the control system described in section 2.2 is shown in Fig. 2. Most
176 of the time the control operates in feedforward mode and the feed rate of solid reactant is
177 proportional to the inlet HCl load. However, when the outlet HCl flowrate exceeds its setpoint,
178 the feedback mode takes over, imposing a relevant excess in feed rate to bring the HCl outlet
179 back under the threshold as soon as possible. This behaviour determines a peak in reactant
180 consumption but generates also unintended instability in the outlet HCl flow rate. As
181 pinpointed by the arrows in Fig. 2, the spike of reactant feed manages to quickly reduce the
182 outlet HCl flow rate, but such a reduction is often followed by a swift rebound of outlet HCl
183 to high values that triggers another activation of the feedback control, resulting in another

spike of reactant feed. Since the layers of solid reactant accumulated over time on the fabric filter are known to play a major role in the overall acid gas removal action (Kim et al., 2017; Wu et al., 2004), the spikes of reactant feed might be detrimental because they induce unstable operation of the filter (Saleem and Krammer, 2012), activating frequent filter cleaning and reducing the residence time of reactant on the filter. The unstable HCl flow rate at the outlet of the 1st stage can in turn disturb the operation of the 2nd stage of acid gas removal.

In general, this control does not include the minimisation of reactant feed as a criterion and does not realise a rational use of reactant.

3 Methodology

3.1 Framework

Fig. 3 summarises the methodology developed to analyse the performance of alternative process control strategies for DSI, aimed at environmental and economic optimisation. The core element of the methodology is the development of a process simulation that allows exploring alternative control settings in a virtual console, while reducing the need for full-scale test-runs at the real plant. The process simulation duplicates into a software environment the process units and the control system of the actual facility. As sketched in Fig. 3, building the simulation required: i) to reproduce the HCl removal process with a process model; and ii) to simulate the control structure of the DSI unit. The first task required the identification of an appropriate mathematical model for the description of the reaction process (see section 3.2) and its training and validation on plant data collected from test-runs

(see section 3.3). The second task was performed replicating the control architecture of the plant, briefly outlined in section 2.2, with a Simulink block diagram (see section 3.4).

The reliability of the simulation is validated considering the operating process control set-up in the real plant and comparing the outputs of the simulation with those recorded in the plant during normal operation, using the actual data as the input for the simulation. Once validated, the simulation can be used to screen and tune alternative control strategies, eventually leading to a new tuned control strategy that may be tested in the real plant, as in the test case that will be introduced in section 4.

Besides conventional indicators of process control performance, specific environmental and economic indicators (section 3.5) were defined to allow a comprehensive assessment of the performance of the alternative control strategies.

3.2 Selection of data-driven process model and input variables

As mentioned above, a mathematical model is required to reproduce the process dynamics in the simulation. The process model needs to predict how the instantaneous HCl removal efficiency varies depending on the inlet HCl concentration and the feed of solid reactant. Given the intrinsic unsteady nature of the process, this task can be addressed only with a dynamic model capable of handling the rapidly changing operating conditions (e.g. variability of HCl concentration due to variability of waste composition). Existing simplified stationary models of acid gas removal that are typically applied for process optimisation studies (Harriott, 1990; Dal Pozzo et al., 2016) are clearly not apt for this task. On the other hand, phenomenological models (Antonioni et al., 2016; Foo et al., 2017; Montagnaro et al., 2016) that describe rigorously the kinetic and mass transfer phenomena involved in the gas-solid reaction process were typically derived from laboratory-scale data and are not suitable to

simulate full-scale systems, as stated by Gutiérrez Ortiz and Ollero (2008) and Gassner et al. (2014).

Therefore, a data-driven approach was chosen. A system identification procedure was performed to estimate the structure and the parameters of the model from observed input-output plant data (Ljung, 2010). A simple input-output polynomial model, *i.e.* the linear auto-regressive exogenous (ARX) model, was selected as base for the system identification. ARX models have already demonstrated to be reliable tools in emission control problems, e.g. in the prediction of NO_X (Smrekar et al., 2013) or SO_X (Choi et al., 2002) emissions from coal-fired boilers. They are appreciated for their transparency and ease of interpretation (Akinola et al., 2019). The general form of an ARX model is the following:

$$y(t) = a_1 y(t-1) + \cdots + a_{n_a} y(t-n_a) + \sum_i \left[b_{1,i} u_i(t-n_k) + \cdots + b_{n_{b,i}} u_i\left(t - n_{k,i} - n_{b,i} + 1\right) \right] + e(t) \quad (4)$$

where y is the output variable, u_i are the i input variables considered in the model, and e is the white-noise disturbance value. The values a and b are the model parameters, which can be represented in compact form in the parameter vector θ:

$$\theta = \left[a_1 \cdots a_{n_a}\ b_{1,i} \cdots b_{n_{b,i}}\ \right]' \quad (5)$$

This model structure implies that the output variable y at time t is predicted as a linear combination of past output values (autoregressive part of the model) and current and past values of the input variables (exogenous part of the model). The parameters n_a and $n_{b,i}$ are, respectively, the number of past output samples and the number of past input samples (for each input variable i) considered for the prediction of the current output. The model can also

consider input delay terms $n_{k,i}$, i.e. the number of input samples that occur before the input affects the output (also known as the dead time of the system). The use of past observations in the prediction of the output allows approximating also derivative terms by difference quotients, thus enabling the reproduction of the dynamics of the modelled system. The numbers n_a, $n_{b,i}$ and $n_{k,i}$ are known as hyperparameters and represent the order of the model, *i.e.* they indicate the number of parameters to optimise in the training of the model.

For the sake of simplicity, a two-input single-output ARX model was chosen for the present study. The modelled output y is the HCl molar flowrate in the flue gas leaving the DSI system. The two input variables u_i are the inlet HCl molar flowrate and the molar flowrate of $Ca(OH)_2$ fed to the DSI system.

In general, other variables might also affect the HCl removal process. The second most abundant acid compound in WtE flue gases, SO_2, can consume a fraction of the reactant feed (Zhang et al., 2019). Fluctuations in the flue gas flowrate can influence reactant residence time (Hunt and Sewell, 2015). Variations in the operating temperature of the HCl removal stage, e.g. caused by fouling in the heat recovery section upstream, can alter the gas-solid reaction kinetics (Dal Pozzo et al., 2018c). However, variations of temperature and flue gas flowrate are typically limited (see Fig. 2d and 2e) and, in the WtE plant under study, the inlet SO2 concentration was a couple of orders of magnitude lower than that of HCl. Therefore, these variables were excluded in the formulation of the model.

3.3 Calibration of the model

As a data-driven model, the ARX structure requires a specific calibration on data from the actual DSI system modelled. Informative data can be obtained by open-loop tests, in which

the control of the system is deactivated and process performance is assessed by varying manually the feed rate of reactant while recording inlet and outlet HCl concentration.

The dataset Z^N, formed by N consecutive observations of the input and output variables, obtained from the tests has to be divided in: i) a training set Z_{trn}, used for the estimation of the optimal model parameters; and, ii) a cross-validation set Z_{crv}, used for the selection of the optimal order of the model.

A further validation data set, Z_{val}, obtained collecting operating data from the normal, closed-loop operation of the DSI system can be used for the assessment of the performance of the trained model.

Denoting as $\hat{y}(t|\theta)$ the output prediction of the model, least-square method is used to estimate the parameter vector θ^* that produces the best fit of the training data Z_{trn}:

$$\theta^* = \arg\min\{V(\theta, Z_{trn})\}, \qquad \text{where } V(\theta, Z_{trn}) = \frac{1}{N_{trn}} \sum_{t=0}^{N_{trn}-1} \big(y(t) - \hat{y}(t|\theta)\big)^2 \qquad (6)$$

The cross-validation compares the performance of models with different orders, each with its optimal parameter vector θ_i^*, estimated from the training set. The best model is the one for which $V(\theta, Z_{crv})$ is the smallest. This procedure helps selecting a model structure without unnecessary complexity (*i.e.* order), as excessively complex models tend to overfit the training set and perform poorly in the cross-validation set. Lastly, the model with order and parameters optimised for the Z_{trn} and Z_{crv} sets can be tested on the validation set Z_{val} and the procedure can go on iteratively until a given threshold of performance is fulfilled.

3.4 Virtual console

The process model described in section 3.2 was integrated into a simulation environment, where also the control loop and the other components of the DSI system were cloned as in

300 the real plant. The virtual console simulating the operation of the real DSI system consists of
301 four blocks, as shown in Figure 4.
302 The block "*Data import*" defines the inlet conditions of the simulation (inlet HCl concentration
303 and flue gas flowrate). These may be either actual plant data, collected at the measurement
304 point PM1 (see Fig. 1), or artificial data, created to test the system performance under specific
305 strain.
306 The input data of the "*Data Import*" block are then transferred to the *"DTS"* and *"DCS"* blocks.
307 The "*DTS*" block contains the process model described in section 3.2. The "*DCS*" block
308 simulates the control system described in section 2.2. Specifically, given as input signals the
309 HCl load at the inlet of the DTS (provided by the "*Data Import*" block) and the HCl load at the
310 outlet of the dry treatment system (modelled by the "*DTS*" block), this block evaluates with a
311 clock time of 1 s the command input for the actuator that regulates the feed rate of $Ca(OH)_2$.
312 The "*Actuator*" block simulates the operation of the screw feeder installed in the real plant.
313 The virtual actuator receives a percentage command of rotational speed calculated by the
314 "*DCS*" block and transforms it into a molar feed rate of solid reactant to the "*DTS*" block,
315 following a linear relationship between percentage command and feed rate that is
316 characteristic of the real feeder. The response of the actuator was modelled as a first order
317 transfer function:
318
319 $$G(s) = \frac{R}{T_m \cdot s + 1} \quad (7)$$
320
321 where T_m is the actuation time of the screw feeder and R is the command to feed rate ratio.

This console allows the comparative testing of the behaviour of the DSI system under the default control (section 2.2) or an alternative control, as discussed in the test case described in section 4.

3.5 Performance indicators selected to test alternative control strategies

Both conventional indicators for process control performance and specific indicators capturing the environmental and economic performance of the process were defined to allow a comparison of alternative control strategies. The indicators are reported in Table 1 alongside their values obtained for the test case that will be introduced in section 4.

With respect to conventional process control indicators, these address the stability of the output variables. The *instability of reactant injection*, expressed as the ratio of the CV of reactant injection to the CV of inlet HCl mass flow, measures the time variability of the feed rate of reactant imposed by the control system. All things equal, a control demanding less variable feed rates is preferred as it induces less mechanical stress on the feeding system. The *instability of HCl outlet*, expressed as the ratio of the CV of outlet HCl mass flow to the CV of inlet HCl mass flow, measures the variability of the HCl mass flow at the outlet of the DSI system.

Environmental indicators trace the material streams responsible for the indirect environmental burdens of HCl removal: the *specific consumption of reactant*, expressed as mass of reactant injected per mass of removed HCl, and the *specific generation of residues*, expressed as mass of process residues generated per mass of removed HCl. These indicators were monitored both for the Ca-based 1st stage and the bicarbonate-fed 2nd stage of HCl removal, as the stabilisation of control in the 1st stage (object of the study) can also result in a more stable operation for the 2nd stage. Therefore, an indicator of *overall generation of*

346 *residues*, encompassing both treatment stages, was also considered to have a complete
347 picture of the environmental benefit of control optimisation.
348 Lastly, an indicator addressing *overall operating costs* was also estimated, by translating the
349 streams of reactants and residues in operating costs considering their unit costs (see Table
350 S1).
351

352 # 4 Test Case

353

354 ## 4.1 Definition of the test case

355 The test facility described in section 2.1 was used to define a test case for the application of
356 the methodology outlined in section 3. An open-loop test-run was used for the calibration of
357 the ARX model, while the accuracy of the resulting virtual console in reproducing the system
358 behaviour under its default control was assessed using several datasets available for the
359 normal operation of the DSI system. An example of alternative control was proposed, tuned
360 in the virtual console, then tested by full-scale test-runs on the real plant. The set of indicators
361 defined in section 3.4 was adopted to quantify the improvements in the stability of process
362 control and the economic and environmental performance.
363

364 ## 4.2 Calibration of the model and validation of the simulation for the test case

365 The behaviour of the DSI system of the test facility was studied via step-response tests (Liu
366 and Gao, 2012). Input excitations were applied to the system by varying stepwise the feed
367 rate of $Ca(OH)_2$. The effect on system behaviour was recorded by continuous monitoring (30
368 s resolution time) of the outlet HCl concentration (measurement point PM2 in Fig. 1), while
369 the inlet HCl concentration was also recorded (measurement point PM1 in Fig. 1).

On the basis of the discussion provided in section 3.2, the ARX model was calibrated considering the molar flowrate of inlet HCl (calculated from the measured inlet HCl concentration and inlet flue gas flowrate) and the feed rate of $Ca(OH)_2$ as input variables, while the molar flowrate of outlet HCl (product of the measured outlet HCl concentration and outlet flue gas flowrate) is the modelled output.

The virtual console including the calibrated process model was then validated, comparing its simulated outlet of HCl with the measured values in four datasets of operation of the DSI system under the reference control, provided the same input data (see section 5.1). The simulation error was quantitatively assessed by calculating a cumulative normalised root mean squared error (RMSE):

$$Normalised\ RMSE\ (t) = \frac{\sqrt{\frac{1}{n(t)}\sum_{i=1}^{n(t)}(y_i - \hat{y}_i)^2}}{\frac{\sum_{i=1}^{n(t)} y_i}{n(t)}} \quad (8)$$

where *n(t)* is the number of measurements/model evaluations at a given time.

4.3 Selection and tuning of an alternative control

Once the accuracy of the simulation results was demonstrated, the virtual console was used to test alternative approaches to the control of HCl removal operation. In this test case, the control logic described in section 2.2 (named in the following as “conventional control”) was substituted with a simple feedback control (named in the following as “alternative control”). Recalling Fig. 2, the conventional control is built to suppress any overrun of the setpoint of outlet HCl concentration with a spike of $Ca(OH)_2$ feed. The consequences of such approach, as illustrated in section 2.3, are an excess consumption of $Ca(OH)_2$ and unstable inlet conditions for the 2nd HCl removal stage fed with $NaHCO_3$, which, again, lead typically to an

392 excess consumption of $NaHCO_3$. Conversely, a properly tuned control in purely feedback
393 action could limit the variability of both reactant feed and outlet HCl concentration.
394 The proposed feedback control is a simple proportional integral (PI) control. As the HCl inlet
395 concentration signal is by nature highly variable and vulnerable to noise contamination
396 (Coleman et al., 2019), the introduction of a derivative (D) control term was avoided, as it
397 could generate system instability (Ting et al., 2008).
398 Hence, in the simulation the two parameters of the feedback control, K_P gain and τ_I integral
399 time, were tuned. The values of the optimised parameters were K_P = 2 and τ_I = 345 s.
400
401 **4.4 Performance assessment of the new control at the real plant**
402 Eventually, a comparative assessment of the performance of the conventional and alternative
403 control was carried out at the test facility. The alternative control was easily implemented, by
404 deactivating the feedforward control and updating the feedback settings to the tuned
405 parameters.
406 The test consisted in comparing a period of DSI process operation with the alternative control
407 with a period of operation with the conventional control. The HCl load released by waste
408 combustion can vary widely over time, and any control logic would manage better a low and
409 uniform inlet mass flow of HCl, rather than a high and fluctuating one. Thus, to ensure a
410 proper comparison, a period of operation experiencing an almost equal inlet mass flow of HCl
411 to that present during the test of the alternative control was selected as representative of the
412 conventional control performance.
413 As a measure of variability of inlet HCl load, the coefficient of variation (CV) of the HCl mass
414 flow during the test period was estimated:
415

$$CV = \frac{\sigma}{\mu} \quad (9)$$

where σ and μ are respectively the standard deviation and the mean of the measurements of inlet HCl mass flow during the period of study. It was also ensured that the two periods of DSI operation used for the comparison exhibited a similar CV of HCl mass flow, as it will be discussed in section 5.3. The HCl removal efficiency *X* was also calculated as follows:

$$X = \frac{\dot{m}_{HCl,in} - \dot{m}_{HCl,out}}{\dot{m}_{HCl,in}} \quad (10)$$

The comparison among the performance of the alternative control strategies was carried out calculating the indicators discussed in section 3.5.

5 Results and Discussion

5.1 Results of the validation of the simulation

Figure 5 reports the performance of the virtual console in simulating the behaviour of the conventional process control of the DSI system on a sample dataset (other samples are shown in Figures S1-S3 in the Supporting Information, SI). The percentage command to reactant feed given by the real system and by the simulation are compared in Fig. 5a. Figure 5b compares the measured and the simulated outlet HCl mass flow. The yellow curve represents the set value of outlet HCl mass flow, which is a fluctuating value as it is defined as the product of the fixed setpoint of outlet HCl concentration (see e.g. Fig. 2b) and the variable value of the flue gas flowrate (see e.g. Fig. 2d). Again, it can be noticed that the conventional control treats the set value more like a threshold than a setpoint, as discussed in section 2.3. Figure 5c plots the cumulative average error of the simulation, represented as a normalised RMSE (introduced in section 4.2). The error increases over time, indicating a loss of performance of the process

model nested in the simulation, that is typical of error accumulation in models of autoregressive nature (Bazghaleh et al., 2013; Nelles, 2020). As evidenced also by the figures in the SI, the error grows faster when outlet HCl fluctuates widely, while it remains almost unchanged and may even decrease during periods of stable operation. It is clear that a simple ARX model, linear by nature, falls short of achieving an accurate instantaneous prediction of HCl outlet, which is the result of a complex and non-linear process involving gas-solid reactions both in duct and on filter bags. Nonetheless, the simulation captures the average system behaviour with acceptable resolution for the objective of the study.

5.2 Results of the virtual testing of the alternative control

The simulation was used for the tuning and for the virtual testing of the alternative PI control. The tuning of the alternative control by the methodology outlined in section 4.3 provided the following value for the control parameters: proportional gain K_P = 2 and integral time τ_I of 345 s. It should be recalled that the PI settings of the feedback component of the conventional control (see section 2.2) are K_P = 5 and τ_I = 8 s. The alternative control is less aggressive, with a reduced proportional action and a significantly higher integral time, which lowers the sensitivity of the control action to temporary deviations of the inlet HCl load. Figure 6a illustrates the different behaviour of the alternative control strategy compared to the conventional process control, on a data sample of 100 min. The simulation of the alternative control was started during a significant deviation of the measured HCl outlet concentration from the set-point value to emphasise the different mode of operation of the two control strategies. The feed rate variations imposed by the alternative control strategy are markedly smoother than those of the conventional control. The proposed strategy accepts momentary upticks in the HCl outlet concentration, whereas the action of the original control results in

463 spikes of reactant feed. Conversely, the alternative control strategy imposes a slightly higher
464 feed rate than the original control during periods in which the latter operates in the
465 feedforward mode. These opposite behaviours are evident from the plot of cumulated
466 reactant consumption reported in Fig. 6c. Given that the variability of the reactant feed rate
467 has been highlighted in section 2.3 as one of the main causes of inefficient reactant
468 exploitation in the DTS, the alternative control strategy appears well suited to rationalise the
469 use of the reactant, thus minimising the resulting generation of process residues.
470
471 **5.3 Results of the field test of the alternative control**
472 The alternative PI control was implemented in the DCS of the test facility. As outlined in
473 section 4.4, a test run of the new control was carried out and the resulting operational data
474 were compared with a previous period under the conventional process control configuration.
475 The equivalence of action between the two controls was guaranteed by selecting the average
476 value of outlet HCl concentration in the previous day under the conventional control as the
477 setpoint for the test of the alternative control (see Fig. 7b).
478 Two 5-hour data samples with similar inlet flue gas conditions were selected for the
479 comparative assessment. The two time series are shown in Fig. 7a, where it is possible to
480 compare qualitatively the behaviour of the two control strategies, i.e. the feed rate of
481 reactant and the outlet HCl flowrate, depending on the inlet HCl flowrate. The relative
482 performance of the two controls was tracked via the indicators introduced in section 3.5.
483 Table 1 provides the list of the indicators used and the specific values obtained, while Figure
484 7c shows a radar plot comparing the normalised values of the performance indicators of the
485 alternative control to the reference one. Internal normalisation was used to obtain the values
486 shown in the figure. Given the low inlet SO_2 concentrations measured at the plant (in the

range 10 – 30 mg/Nm^3) and the relatively low reactivity compared to HCl, the effect of SO_2 on system performance is negligible and not discussed in the analysis.

First of all, the two 5-hour data samples present highly comparable inlet HCl loads, hence the two controls are tested in a situation of similar stress. As reported in Table 1, the average inlet HCl mass flow rate in the two periods is equal and its CV is 68% higher during the test of the alternative control, i.e. the selection of data samples is slightly biased in favour of the conventional control.

Figure 7 shows that the real behaviour of the proposed PI-only control is in line with what was expected from the virtual simulation (see Fig. 6). The feed rate varies smoothly, with slow corrections in face of any sharp variation in the outlet HCl flow. Conversely, the conventional control reacts aggressively to deviations in the HCl outlet, with the characteristic spikes of reactant feed rate already described in Fig. 2.

When the performance indicators introduced in section 3.5 are considered, the parameter instability of reactant injection captures numerically this difference: while the commanded feed rate of the original control shows a CV that is 4.3 times higher than the CV of the inlet HCl molar flow, the CV of the commanded feed rate of the proposed control is only 1.24 times higher (a 71% reduction, see Table 1).

At the same time, the specific consumption of reactant in the $Ca(OH)_2$-fed treatment stage is 11% lower with the proposed control. This confirms that the lower aggressivity of the new control settings is not detrimental to the HCl removal efficiency of the system. On the contrary, in the test period, the proposed control managed to achieve the desired HCl removal performance with a significantly lower variability of reactant feed rate, which has the further advantage of reducing the mechanical stress to the screw feeder and the reactant transport system.

Another relevant metric is the instability of the outlet HCl flow, defined in section 3.5 as the ratio between the CVs of outlet and inlet HCl molar flow. The proposed PI-only control achieves a 39% reduction in this indicator. This means that the HCl load exiting the $Ca(OH)_2$-fed treatment stage is less variable in time, thus the downstream $NaHCO_3$-fed stage operates on a less variable HCl inlet and is put in less stressful working conditions. As a consequence, the optimisation of the control in the $Ca(OH)_2$ stage generates also a 26% reduction in the specific consumption of reactant in the subsequent $NaHCO_3$ stage (see again Table 1), whose control was not modified.

The overall consequence of the increase in efficiency owing to the new PI-only control is the reduction in the production of the solid process residues of HCl removal via both the gas-solid reactions with $Ca(OH)_2$ and $NaHCO_3$. The new control achieves a 7% and a 22% reduction in the generation of process residues, respectively in the 1st and 2nd treatment stages. The overall effect is a 13% reduction of the amount of process waste generated by the HCl removal operation. A further confirmation of this effect can be observed in figure S4 in the SI, which shows the simulated action of the conventional control system considering the inlet HCl load for the 5-hour dataset collected during the test-run. The figure evidences that the multiple activations of the feedback mode would have caused a higher reactant consumption.

5.4 Discussion

In the light of the indicators in Table 1, the alternative control strategy tuned in the virtual simulation was demonstrated to improve the overall economic and environmental performance of the system. The consumption of reactants and the generation of process residues were lowered in both the treatment stages, by increasing the efficiency of reactant delivery. It was thus demonstrated that the main drawback of dry acid gas removal, i.e. the

required high excess of reactant, can be partially mitigated by introducing specific process control strategies. In particular, for a multistage system as that of the test facility, it is worth highlighting that an intervention limited to the 1st treatment stage can produce benefits also on the 2nd stage, by enabling a more efficient operation thanks to the lowered variability of the inlet HCl.

The alternative control strategy, based on a PI feedback control, however, has clear limitations: even if the simple feedback action reduces the variability of HCl load compared to the conventional control, the instability with respect to a setpoint is still quite high. More advanced control strategies could offer further improvements. Nonetheless, the proposed solution achieved the results in Table 1 with minimal need of full-scale testing and no significant change in the control architecture of the system, demonstrating the ease of implementation of better solid waste and reactant management via control optimisation.

The results obtained show that the procedure developed for the test of alternative control strategies, based on a virtual console, and the metric introduced, based on the performance indicators listed in Table 1, provide an effective approach to allow the improvement of the environmental and economic operational performance of acid gas treatment systems.

6 Conclusions

With increasingly strict limits on the emission of airborne pollutants as HCl, the flue gas treatment sections in WtE installations are experiencing problems of excessive consumption of reactants and related high generation of solid residues destined to landfilling, which lead to non-negligible indirect environmental burdens. By considering a reference state-of-the-art acid gas removal system, the present study demonstrated that a standard process control

approach based exclusively on the suppression of HCl emissions might be a suboptimal solution in terms of economic and environmental performance. A simple methodology based on virtual simulation and limited full-scale test-runs allowed identifying and tuning an alternative control strategy that achieved a reduction in the generation of solid process residues equal to 7% in the optimised $Ca(OH)_2$-fed 1st stage of HCl removal and 13% in the overall two-stage treatment line with respect to the original control configuration, while maintaining the same HCl emission performance at stack.

Despite the relevant advantages in terms of reactant economy, a limitation of the proposed solution is that it only partially alleviates the fluctuations in the HCl concentration at the outlet of the 1st treatment stage, which are intrinsic to the WtE context. More advanced process control strategies, taking into account process disturbances other than inlet pollutant concentration and reactant feed rate, could be the key to develop plant-specific highly performant model-based control schemes. However, the present study evidenced that process control optimisation is a promising area of improvement in the management of WtE flue gas treatment, not only to improve stable operation, but also to increase significantly the economic and environmental performance of DSI processes without hindering the compliance to emission limits at stack.

References

Akinola, T.E., Oko, E., Gu, Y., Wei, H.-L., Wang, M., 2019. Non-linear system identification of solvent-based post-combustion CO2 capture process. Fuel 239, 1213-1223.

Antonioni, G., Dal Pozzo, A., Guglielmi, D., Tugnoli, A., Cozzani, V., 2016. Enhanced modelling of heterogeneous gas-solid reactions in acid gas removal dry processes. *Chem. Eng. Sci.* 148, 140-154.

Ardolino, F., Boccia, C., Arena, U., 2020. Environmental performances of a modern waste-to-energy unit in the light of the 2019 BREF document. Waste Manage. 104, 94-103.

Arena, U., 2015. From waste-to-energy to waste-to-resources: The new role of thermal treatments of solid waste in the Recycling Society. Waste Manage. 37, 1-2.

Bagheri, M., Esfilar, R., Golchi, M.S., Kennedy, C.A., 2020. Towards a circular economy: A comprehensive study of higher heat values and emission potential of various municipal solid wastes. Waste Manage. 101, 210-221.

Bal, M., Reddy, T.T., Meikap, B.C., 2019. Removal of HCl gas from off gases using self-priming venturi scrubber. J. Haz. Mat. 364, 406-418.

Bazghaleh, M., Mohammadzaheri, M., Grainger, S., Cazzolato, B., Lu, T.-F., 2013. A new hybrid method for sensorless control of piezoelectric actuators. Sensors and Actuators A: Physical 194, 25-30.

Beylot, A., Hochar, A., Michel, P., Descat, M., Ménard, Y., Villeneuve, J., 2018. Municipal Solid Waste Incineration in France: An Overview of Air Pollution Control Techniques, Emissions, and Energy Efficiency. J. Ind. Ecol. 22, 1016-1026.

Bogush, A., Stegemann, J.A., Wood, I., Roy, A., 2015. Element composition and mineralogical characterisation of air pollution control residue from UK energy-from-waste facilities. Waste Manage. 36, 119-129.

CEN, 2019. CEN/TS 17337:2019 – Stationary source emissions - Determination of mass concentration of multiple gaseous species - Fourier transform infrared spectroscopy. European Committee for Standardization, Bruxelles, Belgium.

Choi, S., Yoo, C., Lee, I.-B., 2002. SOx monitoring and neural net classification in the power plant. J. Environ. Eng. 128, 911-918.

Cignitti, S., Mansouri, S.S., Sales-Cruz, M., Jensen, F., Huusom, J.K., 2016. Dynamic Modeling and Analysis of an Industrial Gas Suspension Absorber for Flue Gas Desulfurization. Emiss. Control Sci. Technol. 2, 20-32.

Coleman, M.D., Ellison, M., Robinson, R.A., Gardiner, T.D., Smith, T.O.M., 2019. Uncertainty requirements of the European Union's Industrial Emissions Directive for monitoring sulfur dioxide emissions: Implications from a blind comparison of sulfate measurements by accredited laboratories. J. Air Waste Manage. Assoc. 69, 1070-1078.

Dal Pozzo, A., Moricone, R., Tugnoli, A., Cozzani, V., 2019. Experimental Investigation of the Reactivity of Sodium Bicarbonate toward Hydrogen Chloride and Sulfur Dioxide at Low Temperatures. *Ind. Eng. Chem. Res.* 58, 6316-6324.

615 Dal Pozzo, A., Lazazzara, L., Antonioni, G., Cozzani, V., 2020. Techno-economic
616 performance of HCl and SO2 removal in waste-to-energy plants by furnace direct sorbent
617 injection. *J. Haz. Mat.* 394, 122518.

618 Dal Pozzo, A., Guglielmi, D., Antonioni, G., Tugnoli, A., 2018a. Environmental and
619 economic performance assessment of alternative acid gas removal technologies for
620 waste-to-energy plants. *Sust. Prod. Consumption* 16, 202-215.

621 Dal Pozzo, A., Armutlulu, A., Rekhtina, M., Müller, C.R., Cozzani, V. 2018b. CO2 Uptake
622 Potential of Ca-Based Air Pollution Control Residues over Repeated Carbonation-
623 Calcination Cycles. *Energy Fuels* 32, 5386-5395.

624 Dal Pozzo, A., Giannella, M., Antonioni, G., Cozzani, V., 2018c. Optimization of the
625 economic and environmental profile of HCl removal in a municipal solid waste incinerator
626 through historical data analysis. *Chem. Eng. Trans.* 67, 463-468.

627 Dal Pozzo, A., Guglielmi, D., Antonioni, G., Tugnoli, A., 2017. Sustainability analysis of dry
628 treatment technologies for acid gas removal in waste-to-energy plants. *J. Clean. Prod.* 162,
629 1061-1074.

630 Dal Pozzo, A., Antonioni, G., Guglielmi, D., Stramigioli, C., Cozzani, V., 2016. Comparison
631 of alternative flue gas dry treatment technologies in waste-to-energy processes. *Waste*
632 *Manage.* 51, 81-90.

633 Damgaard, A., Riber, C., Fruergaard, T., Hulgaard, T., Christensen, T.H., 2010. Life-cycle-
634 assessment of the historical development of air pollution control and energy recovery in
635 waste incineration. *Waste Manage.* 30, 1244-1250.

636 De Greef, J., Villani, K., Goethals, J., Van Belle, H., Van Caneghem, J., Vandecasteele, C.,
637 2013. Optimising energy recovery and use of chemicals, resources and materials in
638 modern waste-to-energy plants. Waste Manage. 33, 2416-2424.

639 Dong, J., Jeswani, H.K., Nzihou, A., Azapagic, A., 2020. The environmental cost of
640 recovering energy from municipal solid waste. Appl. Energy 267, 114792.

641 Ephraim, A., Ngo, L.D., Pham Minh, D., Lebonnois, D., Peregrina, C., Sharrock, P., Nzihou,
642 A., 2019. Valorization of Waste-Derived Inorganic Sorbents for the Removal of HCl in
643 Syngas. Waste Biomass Valorization 10, 3435-3446.

644 Foo, R., Berger, R., Heiszwolf, J.J., 2016. Reaction Kinetic Modeling of DSI for MATS
645 Compliance. In: Proceedings of the Power Plant Pollutant Control and Carbon
646 Management “MEGA” Symposium, Baltimore, MD, USA, 16–19 August 2016

647 Gassner, M., Nilsson, J., Nilsson, E., Palmé, T., Züfle, H., Bernero, S., 2014. A data-driven
648 approach for analysing the operational behaviour and performance of an industrial flue
649 gas desulphurisation process. Computer Aided Chem. Eng. 33, 661-666.

650 Gerassimidou, S., Velis, C.A., Williams, P.T., Castaldi, M.J., Black, L., Komilis, D., 2020.
651 Chlorine in waste-derived solid recovered fuel (SRF), co-combusted in cement kilns: A
652 systematic review of sources, reactions, fate and implications. Critical Reviews in
653 Environmental Science and Technology, in press.

654 Goodall, P.; Sharpe, R.; West, A., 2019. A data-driven simulation to support
655 remanufacturing operations. Computers in Industry 105, 48-60.

Guo, Y., Xu, Z., Zheng, C., Shu, J., Dong, H., Zhang, Y., Weng, W., Gao, X., 2019. Modeling and optimization of wet flue gas desulfurization system based on a hybrid modeling method. J. Air Waste Manage. Assoc. 69, 565-575.

Gutiérrez Ortiz, F.J., Ollero, P., 2008. A realistic approach to modeling an in-duct desulfurization process based on an experimental pilot plant study. *Chem. Eng. J.* 141, 141-150.

Harriott, P., 1990. A Simple Model for SO_2 Removal in the Duct Injection Process. J. Air Waste Manage. Assoc. 40, 998-1003.

Hartman, M., Svoboda, K., Pohorely, M., Syc, M., 2013. Thermal Decomposition of Sodium Hydrogen Carbonate and Textural Features of Its Calcines. Ind. Eng. Chem. Res. 52, 10619-10626.

Hunt, G., Sewell, M., 2015. Utilizing Dry Sorbent Injection Technology to Improve Acid Gas Control. In: 34th International Conference on Thermal Treatment Technologies & Hazardous Waste Combustors, Houston, TX, USA, 20-22 October 2015

Iizuka, A., Morishita, Y., Shibata, E., Takatoh, C., Cho, H., 2020. Basic Study of the Reaction of Calcium Hydroxide with Hydrogen Chloride Using Single Crystals. *Ind. Eng. Chem. Res.* 59, 9699-9704.

Kameda, T., Tochinai, M., Kumagai, S., Yoshioka, T., 2020. Treatment of HCl gas by cyclic use of Mg–Al layered double hydroxide intercalated with CO32-. Atmospheric Pollution Res. 11, 290-295.

Kim, K.-D., Jeon, S.-M., Hasolli, N., Lee, K.-S., Lee, J.-R., Han, J.-W., Kim, H.T., Park, Y.-O., 2017. HCl removal characteristics of calcium hydroxide at the dry-type sorbent reaction accelerator using municipal waste incinerator flue gas at a real site. Korean J Chem Eng 34, 747-756.

Kockmann, N., 2019. Digital methods and tools for chemical equipment and plants. Reaction Chemistry and Engineering 4, 1522-1529.

Lausselet, C., Cherubini, F., del Alamo Serrano, G., Becidan, M., Strømman, A.H., 2016. Life-cycle assessment of a Waste-to-Energy plant in central Norway: Current situation and effects of changes in waste fraction composition. Waste Manage. 58, 191-201.

Liu, T., Gao, F., 2012. Step Response Identification of Stable Processes. In: Liu, T., Gao, F., Industrial Process Identification and Control Design, Springer-Verlag London, London, UK.

Liu, S., Sun, L., Zhu, S., (...), Chen, X., Zhong, W., 2020. Operation strategy optimization of desulfurization system based on data mining. Appl. Mathematical Modelling 81, 144-158.

Ljung, L., 2010. Perspectives on system identification. Annual Reviews in Control 34, 1-12.

Margallo, M., Taddei, M.B.M., Hernández-Pellón, A., Aldaco, R., Irabien, A., 2015. Environmental sustainability assessment of the management of municipal solid waste incineration residues: A review of the current situation. Clean Technol. Environ. Policy 17, 1333-1353.

Montagnaro, F., Balsamo, M., Salatino, P., 2016. A single particle model of lime sulphation with a fractal formulation of product layer diffusion. Chem. Eng. Sci. 156, 115-120.

Muratori, G., Dal Pozzo, A., Antonioni, G., Cozzani, V., 2020. Application of Multivariate Statistical Methods to the Modelling of a Flue Gas Treatment Stage in a Waste-to-energy Plant. *Chem. Eng. Trans.* 82, 397-402.

Nelles, O., 2020. Nonlinear System Identification: From Classical Approaches to Neural Networks, Fuzzy Models, and Gaussian Processes. Springer Nature, Berlin, Germany.

Neuwahl, F., Cusano, G., Gomez Benavides, J., Holbrook, S., Roudier, S., 2019. Best Available Techniques (BAT) Reference Document for Waste Incineration. EUR 29971 EN. doi:10.2760/761437

Ouda, O.K.M., Raza, S.A., Nizami, A.S., Rehan, M., Al-Waked, R., Korres, N.E., 2016. Waste to energy potential: A case study of Saudi Arabia. Renewable Sustainable Energy Reviews 61, 328-340.

Peng, H., Ozaki, T., Toyoda, Y., Shioya, H., Nakano, K., Haggan-Ozaki, V., Mori, M., 2004. RBF-ARX model-based nonlinear system modeling and predictive control with application to a NOx decomposition process. Control Engineering Practice 12, 191-203.

Quina, M.J., Bontempi, E., Bogush, A., Schlumberger, S., Weibel, G., Braga, R., Funari, V., Hyks, J., Rasmussen, E., Lederer, J., 2018. Technologies for the management of MSW incineration ashes from gas cleaning: New perspectives on recovery of secondary raw materials and circular economy. Sci. Total Environ. 635, 526-542.

Saleem, M., Krammer, G., 2012. On the Stability of Pulse-Jet Regenerated-Bag Filter Operation. Chemical Engineering and Technology 35, 877-884.

Smrekar, J., Potočnik, P., Senegačnik, A., 2013. Multi-step-ahead prediction of NOx emissions for a coal-based boiler. Appl. Energy 106, 89-99.

Ting, C.-H., Chen, H.-H., Yen, C.-C., 2008. A PID ratio control for removal of HCl/SOx in flue gas from refuse municipal incinerators. Control Engineering Practice 16, 286-293.

Van Caneghem, J., Van Acker, K., De Greef, J., Wauters, G., Vandecasteele, C., 2019. Waste-to-energy is compatible and complementary with recycling in the circular economy. Clean Technol. Environ. Policy, in press.

Vehlow, J., 2015. Air pollution control systems in WtE units: An overview. *Waste Manage.* 37, 58-74.

Wu, C., Kang, S.-J., Keener, T.C., Lee, S.-K., 2004. A model for dry sodium bicarbonate duct injection flue gas desulfurization. Advances in Environmental Research 8, 655-666.

Yang, N., Damgaard, A., Scheutz, C., Shao, L.-M., He, P.-J., 2018. A comparison of chemical MSW compositional data between China and Denmark. J. Environ. Sci. 74, 1-10.

Zhang, H., Yu, S., Shao., L., He, P., 2019. Estimating source strengths of HCl and SO2 emissions in the flue gas from waste incineration. J. Environ. Sci. 75, 370-377.

Figures and Tables

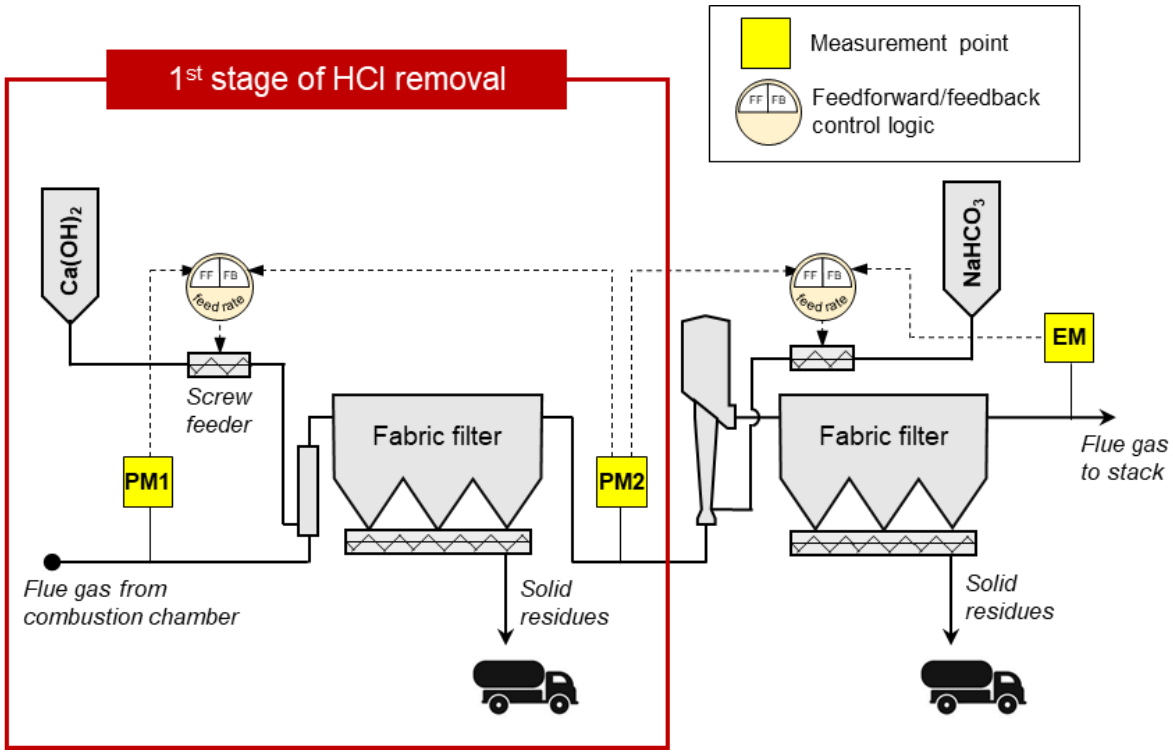

Figure 1. *Scheme of the two-stage acid gas abatement system of the test facility considered, including measurement points of flue gas composition (PM1, PM2 = process measurement, EM = measurement at stack) and control loops for reactant feed rate. Control optimization of 1st stage (red box in the figure) was the object of the study.*

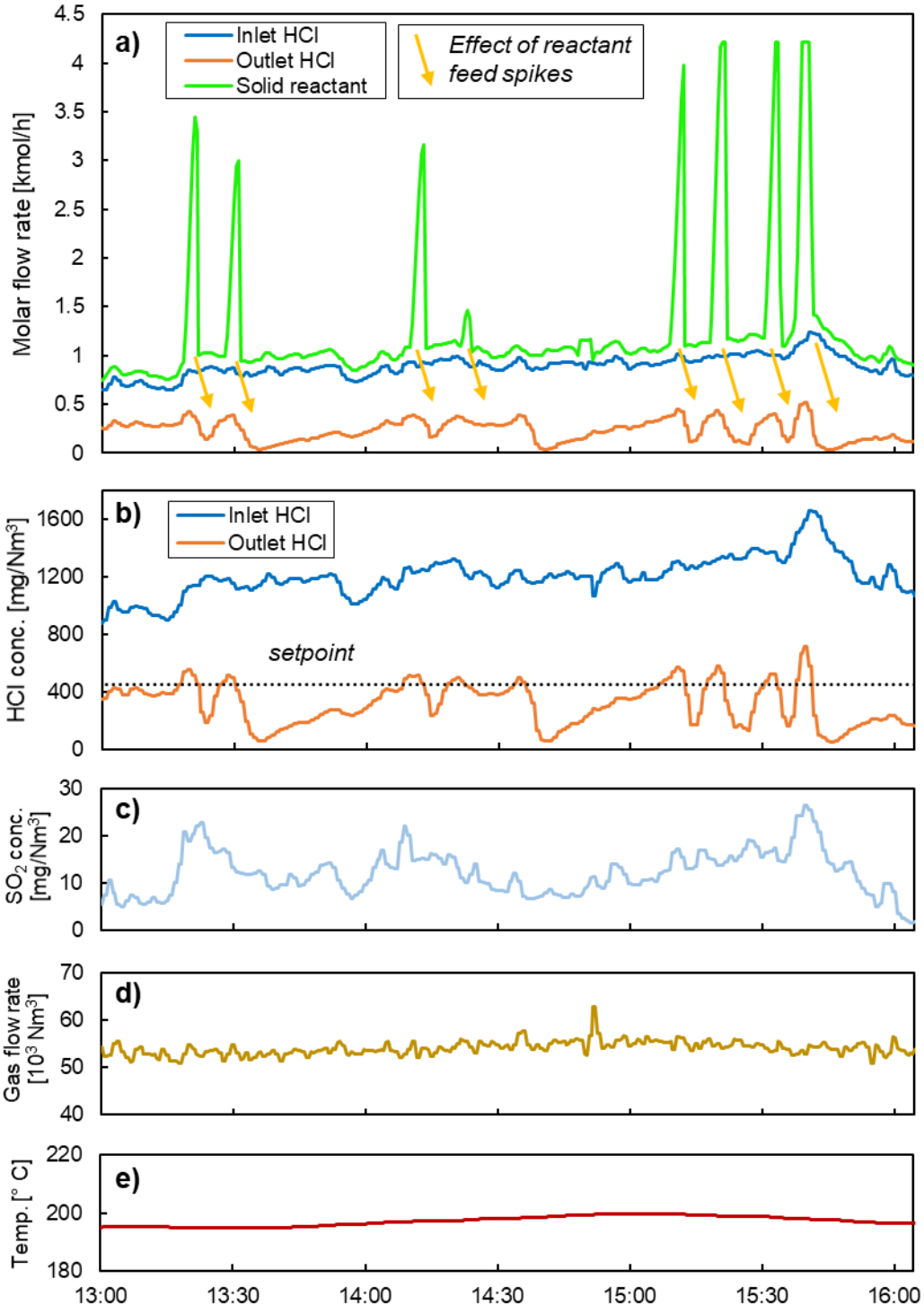

744

745 **Figure 2.** *Data recorded by the distributed control system (DCS) of an Italian WtE facility*
746 *showing: a) the typical trend of inlet and outlet HCl flowrate and solid reactant feed rate*
747 *during normal operation of the 1st stage acid gas removal unit applying the conventional*
748 *process control strategy; b) threshold setpoint with respect to HCl inlet and outlet*
749 *concentrations; c) SO_2 concentration; d) flue gas flowrate; e) operating temperature.*

750

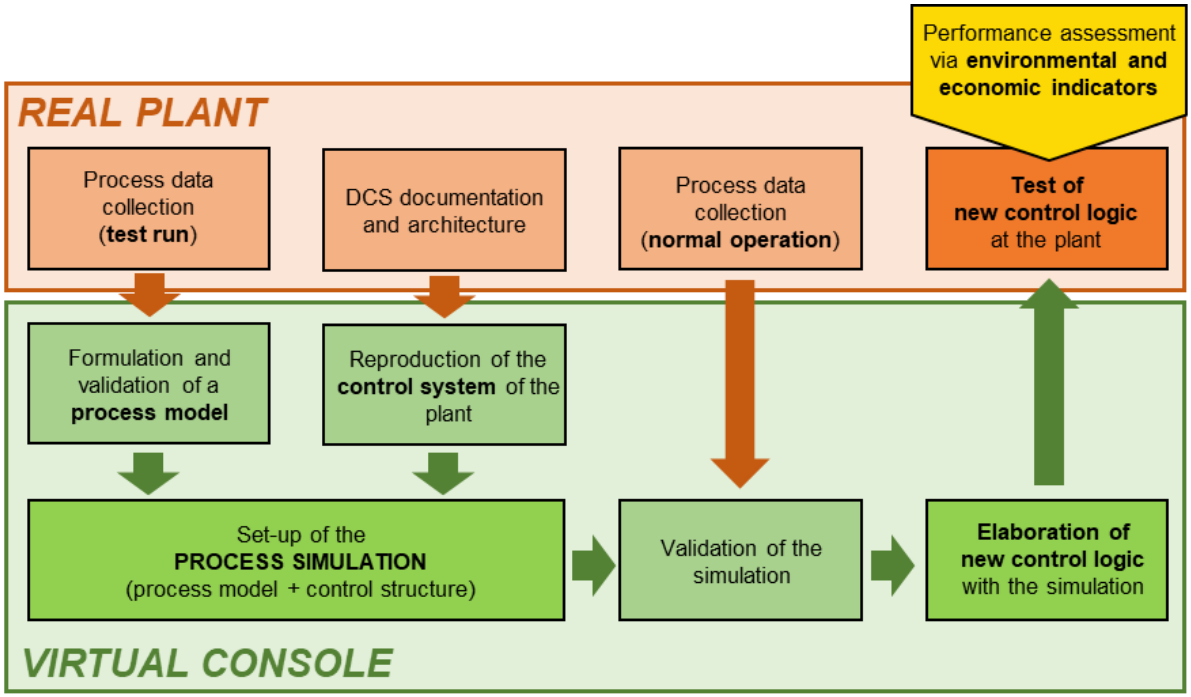

751

752 **Figure 3.** *Methodology developed for testing and tuning of improved process control*

753 *strategies.*

754

755

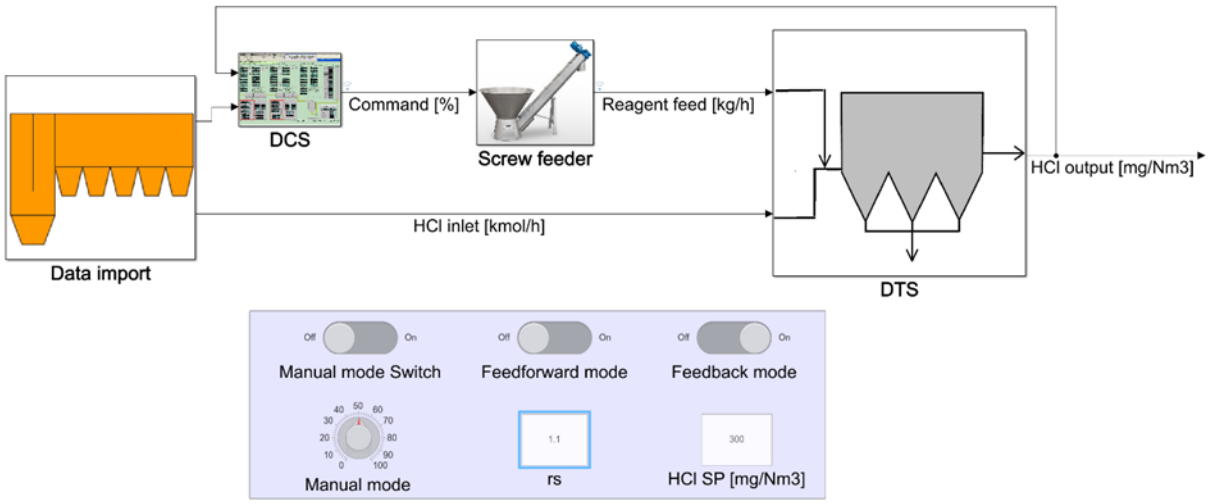

Figure 4. *Virtual console developed to simulate the DSI process (1st stage of the acid gas removal system in Fig. 1) using the Simulink® software tool.*

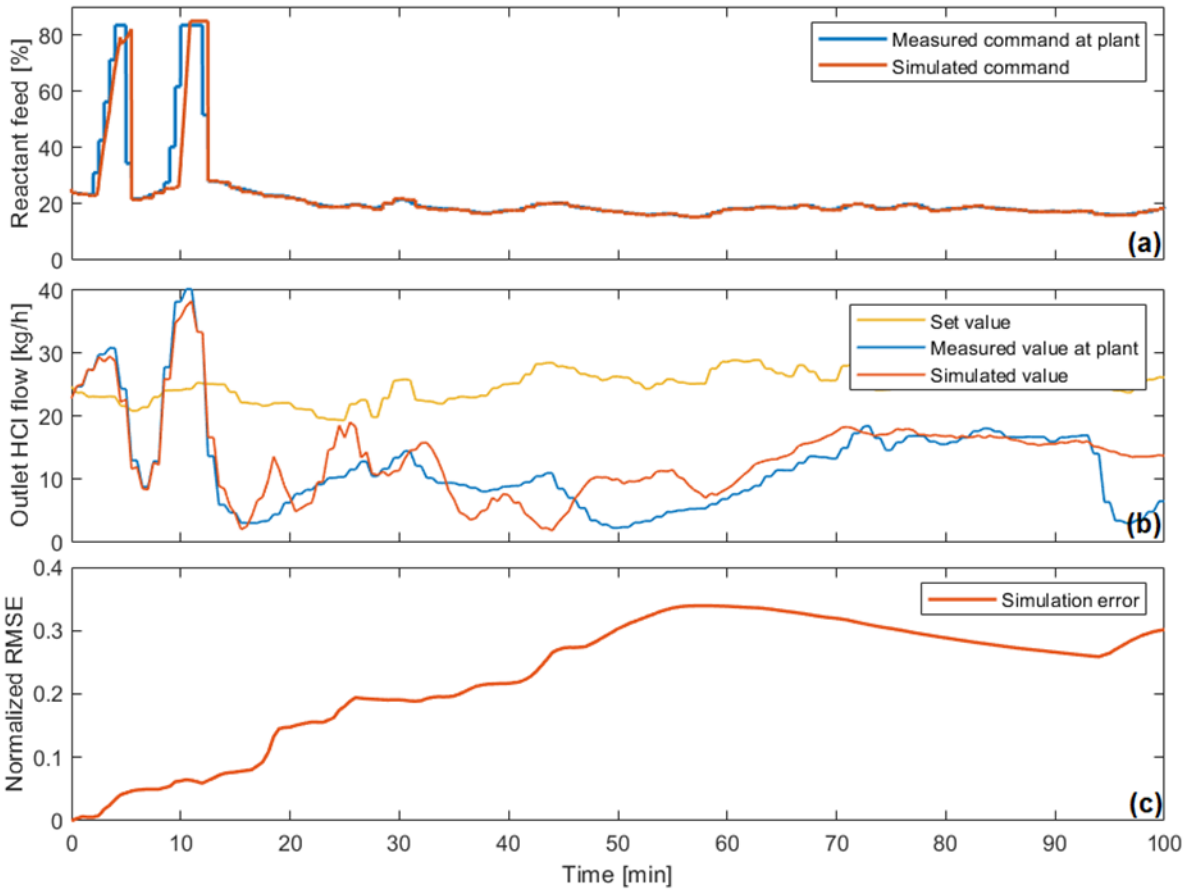

Figure 5. *Performance of the virtual console in simulating the behaviour of the conventional control of the system: a) measured vs. simulated command of reactant feed, b) measured vs. simulated outlet HCl flow rate, compared to the set value of the control, c) cumulative average error of the simulation.*

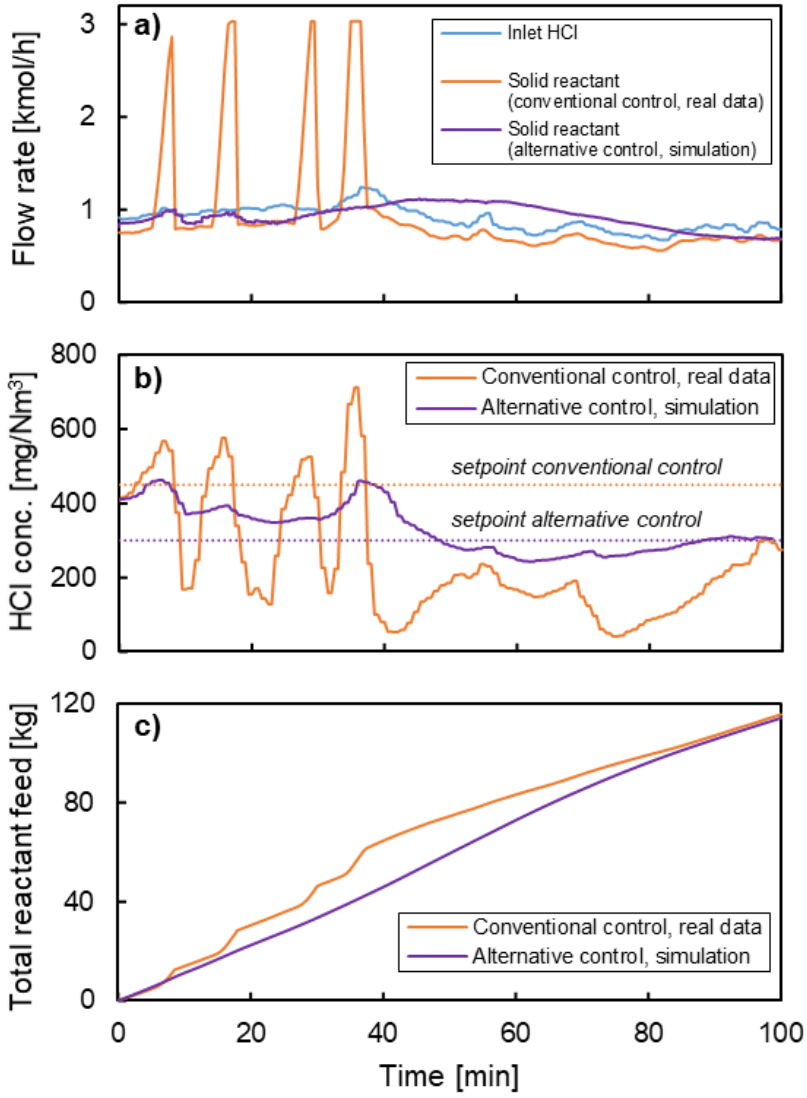

767

768 **Figure 6.** a) *Simulation of the reactant feed rate by the alternative PI control strategy*

769 *compared to the conventional process control on a sample dataset; b) deviation of the outlet*

770 *HCl concentration from the respective setpoints, c) resulting cumulated reactant consumption.*

771

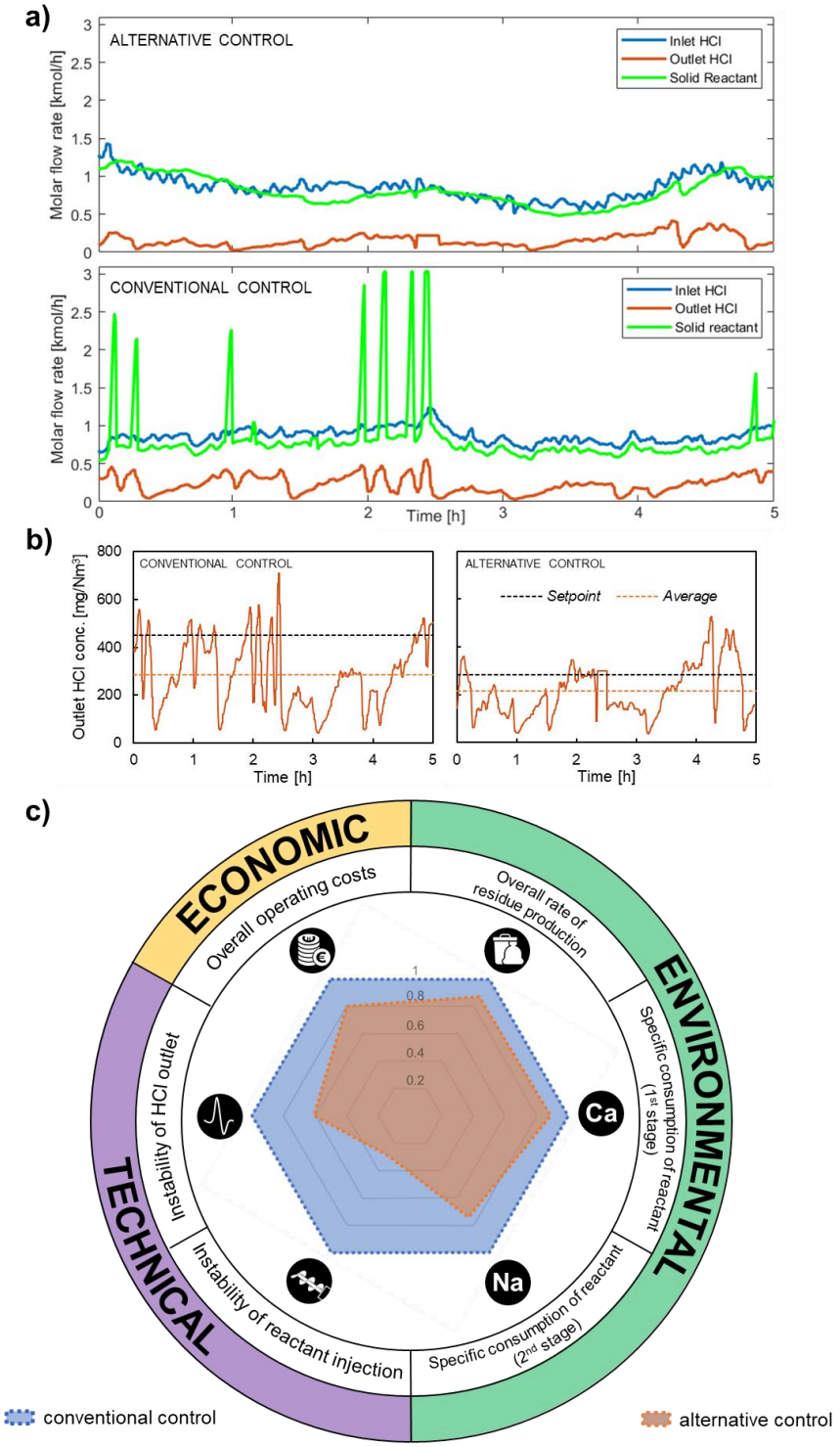

772

773 **Figure 7.** *Results of test-run: a) 5-hour data samples obtained during alternative process*
774 *control and conventional process control operation under a similar HCl input, b) outlet HCl*
775 *concentration in the two 5-hour data samples, c) comparison between the normalised*
776 *performance indicators of the alternative process control strategy to the conventional process*
777 *control.*

778 **Table 1.** *Performance of the alternative control strategy vs. the conventional process control*

779 *monitored according to the performance indicators introduced in section 3.5.*

Parameter or indicator		Test period		Δ
		Conventional control	Alternative control	
Inlet HCl mass flow rate (kg/h)	μ	64.4	64.4	-
	CV	0.12	0.19	+68%
Feed rate of reactant, $Ca(OH)_2$ (kg/h)	μ	61.1	60.0	-2%
	CV	0.49	0.24	-52%
Outlet HCl mass flow rate (kg/h)	μ	17.2	12.5	-27%
	CV	0.51	0.52	+2%
HCl removal efficiency (%)	μ	75.8	82.3	+9%
	CV	11.2	8.5	-24%
Instability of reactant injection (CV of $Ca(OH)_2$ feed rate / CV of inlet HCl)		4.27	1.24	**-71%**
Instability of HCl outlet (CV of outlet HCl / CV of inlet HCl)		4.4	2.7	**-39%**
Specific consumption of reactant (1^{st} stage) (kg of $Ca(OH)_2$ fed / kg of HCl removed)		1.30	1.16	**-11%**
Specific generation of residues (1^{st} stage) (kg of residues / kg of HCl removed)		1.80	1.67	**-7%**
Specific consumption of reactant (2^{nd} stage) (kg of $NaHCO_3$ fed / kg of HCl removed)		3.85	2.86	**-26%**
Specific generation of residues (2^{nd} stage) (kg of residues / kg of HCl removed)		2.55	2.00	**-22%**
Overall rate of residue production (kg of residues / kg of HCl removed)		2.00	1.73	**-13%**
Overall economic performance (€ of operating costs / kg of HCl removed)		1.86	1.48	**-20%**

780

781

Economic and environmental benefits by improved process control strategies in HCl removal from waste-to-energy flue gas

*Alessandro Dal Pozzo, Giacomo Muratori, Giacomo Antonioni, Valerio Cozzani**
LISES - Dipartimento di Ingegneria Civile, Chimica, Ambientale e dei Materiali, Alma Mater Studiorum - Università di Bologna, via Terracini n.28, 40131 Bologna, Italy

(*)*corresponding author*, Tel. +39-051-2090240, Fax +39-051-2090247, e-mail: valerio.cozzani@unibo.it

Abstract

The control of HCl emission in waste-to-energy (WtE) facilities is a challenging flue gas treatment problem: the release of HCl from waste combustion is highly variable in time and the HCl emission standards are typically far lower in WtE than in any other industry. Traditional process control approaches in dry HCl removal processes are generally based on feeding a large excess of solid reactants to the system, to ensure robustness and a wide safety margin in the compliance to environmental regulations. This results in the production of a high amount of unreacted sorbents, strongly increasing the generation of solid wastes that need to be disposed. In the present study, an approach was developed to allow the implementation of improved control strategies for dry HCl abatement systems in operating full-scale facilities. Its objective is the reduction of the reactant feed and the waste production, while still providing an adequate safety margin for emission compliance. The approach was based on the reproduction of the behaviour of the real system in a virtual console that allows the extensive testing of alternative control strategies, limiting the need of demanding test-runs at the real plant. A test case on an Italian WtE facility demonstrated the capability of a control logic tuned in the virtual console to achieve a 13% reduction in the consumption of reactants and generation of process residues, with unchanged HCl removal

efficiency. The results evidence the wide opportunities for optimisation of dry acid gas removal systems, in particular when multistage systems are implemented.

Keywords: waste-to-energy, HCl, process optimization, dry sorbent injection.

1 Introduction

In a modern waste management system, waste-to-energy (WtE) facilities have the role to divert from landfilling waste streams for which recycling is currently technically or economically unfeasible (Nizami et al., 2016) and enabling their thermal valorisation (Arena et al., 2015), thus facilitating the transition to a circular economy (Bagheri et al., 2020; Van Caneghem et al., 2019). Thanks to increasingly ambitious environmental regulations, the emission of several air pollutants related to WtE operation has been reduced more than tenfold in the last decades (Ardolino et al., 2020; Damgaard et al., 2010). However, in the current holistic approach to environmental protection, the reduction of impacts has to go beyond the minimisation of the emission of pollutants at the stack of the plant. Also indirect impacts, e.g. those associated to the consumption of reactants and the production of process residues in the flue gas treatment system of the plant (Dal Pozzo et al., 2017; Dong et al., 2020; Lausselet et al., 2016), needs to be minimised.

Hydrogen chloride (HCl) is a typical pollutant in WtE flue gases, arising from the combustion of waste containing chlorine (Zhang et al., 2019). Chlorine is widely dispersed amongst organic and inorganic compounds present in several waste items (Gerassimidou et al., 2020; Yang et al., 2018). Among the different techniques available for HCl removal (Bal et al., 2019; Dal Pozzo et al., 2019; Ephraim et al., 2019; Kameda et al., 2020), dry sorbent injection (DSI) is one of the technologies more frequently implemented (Beylot et al., 2018; Dal Pozzo et al., 2018a). DSI consists in the in-duct addition of an alkaline powdered reactant (e.g. calcium

hydroxide or sodium bicarbonate), which neutralises acid pollutants as HCl via gas-solid reaction (Antonioni et al., 2016). DSI, adopted in either single or two-stage configurations (Dal Pozzo et al., 2016; De Greef et al., 2013), is considered among the best available techniques for flue gas treatment in WtE installations recommended by the European Union (Neuwahl et al., 2019).

The main environmental drawback of DSI systems is the high stoichiometric excess of reactant feed that is required to achieve high HCl removal efficiency (Vehlow, 2015). The resulting excess consumption of reactant leads to the generation of relevant streams of solid process residues in the fabric filters, where they are collected together with fly ashes and micropollutants. The presence of these other components in the collected process residues causes the stream to be considered as hazardous waste and to require its disposal in dedicated landfill sites (Dal Pozzo et al., 2018b; Kameda et al., 2020).

In addition, given that the composition of the waste burnt in the combustion chamber of a WtE plant varies widely over time, the resulting extreme variability of HCl concentration at the inlet of the flue gas treatment section (Dal Pozzo et al., 2020) is an inherent instability that limits the effectiveness of conventional control strategies in calibrating the reactant feed needed to maintain a constant concentration setpoint at the outlet. Thus, the prevailing trend in control strategies is to calibrate the process control parameters of the DSI system on the safe side, and even more so accept high excess feed rates of reactants to minimise the possible occurrence of overruns of HCl emission limits at stack.

A more accurate setting of the DSI control system could ensure not only a safe compliance of emission limits at stack, but also a reduction of the consumption of reactants and the generation of process residues. These in principle represent an undesired environmental

burden shift between different compartments (from air to soil/water) (Bogush et al., 2015; Margallo et al., 2015; Quina et al., 2018).

The problem of the optimisation of flue gas treatment control with reference either to the WtE context or to acid pollutants (HCl, SO_2, HF) is scarcely addressed in scholarly literature. Ting et al. (2008) described the design of a PID control for acid gas removal via semi-dry scrubbing in a WtE plant, with parameter tuning performed during commissioning operation. Gassner et al. (2014) explored the use of data-driven modelling approaches to describe the non-stationary operational behaviour of a semi-dry flue gas desulfurization process. Cignitti et al. (2016) developed a simple first principle model to predict the dynamics of a semidry SO_2 absorber in desulfurization units of coal-fired power plants, while Guo et al. (2019) used a hybrid approach, blending first principles and neural network, to model and optimise a wet flue gas desulfurization unit. Yet, the focus of these recent studies has been mainly the theoretical development of enhanced dynamic models of the process, rather than their implementation in real control schemes. In particular, to the best of the authors' knowledge, no previous paper addresses the potential environmental and economic advantages in terms of reduced reactant consumption and related waste generation achievable with process control optimisation in WtE acid gas removal.

Furthermore, control optimisation in the WtE context is made complex by the fact that conventional direct tuning via extensive test runs during plant operation is generally incompatible with the need to comply with strict HCl emission limits in presence of a highly variable inlet load of HCl coming from waste combustion. In this regard, the set-up of data-driven simulations of the real system in a virtual environment, as more and more frequently performed in the manufacturing (Goodall et al., 2019) and process industry (Kockmann, 2019), could drastically reduce the need of field tests. By this strategy, the screening and the

98 tuning of new control settings is carried out directly in a virtual set-up, thus limiting the
99 number of in-field test runs only to those needed for the initial calibration of the simulation
100 and for the final trial of the new control system.
101 The present study focuses on the development of an approach for the optimisation of process
102 control in a typical DSI system for HCl removal based on a virtual environment. A dynamic
103 simulation of the dry treatment system was built in a virtual console implemented using the
104 Simulink software. A data-driven process model, calibrated with a specific set of test data,
105 nested into a reproduction of the control system of the DSI unit, was thus obtained and
106 validated. The virtual console was used to test and tune an alternative control strategy, with
107 the objective to reduce the stoichiometric excess of reactant associated to HCl removal. The
108 alternative control was then tested in full scale at the real plant, demonstrating the potential
109 for significant environmental and economic benefits deriving from the reduction in reactant
110 consumption and related process waste generation.
111

2 Reference system and test facility

2.1 HCl removal system

The two-stage acid gas abatement system of a medium-sized (400 t/d of waste treated) WtE facility located in Northern Italy was used as case study. As shown in Fig. 1, this system is based on two consecutive steps of dry sorbent injection and filtration, taking place at ~180 °C, downstream of the heat recovery section of the plant. In the first stage, calcium hydroxide, $Ca(OH)_2$, is injected, triggering the following gas-solid reaction of HCl neutralisation (Iizuka et al., 2020):

$$Ca(OH)_2 + 2\,HCl \rightarrow CaCl_2 + 2\,H_2O \quad (1)$$

A fabric filter separates the solid product of reaction from the flue gas, together with a relevant unreacted fraction of $Ca(OH)_2$, present both due to the excess feed of reactant and for the intrinsic diffusional limitations of gas-solid reaction (i.e. the phenomenon of incomplete conversion discussed by Antonioni et al., 2016). In the second stage, the dry injection is based on sodium bicarbonate, $NaHCO_3$. At the injection temperature and, in general, at T > 130 °C (see Hartman et al., 2013), $NaHCO_3$ decomposes to porous sodium carbonate (Na_2CO_3), which in turn absorbs HCl (Dal Pozzo et al., 2019):

$$2\,NaHCO_3 \rightarrow Na_2CO_3 + CO_2 + H_2O \quad (2)$$

$$Na_2CO_3 + 2\,HCl \rightarrow 2\,NaCl + CO_2 + H_2O \quad (3)$$

Again, the solid product of reaction and an unreacted fraction of reactant are collected by a fabric filter. This two-stage configuration is adopted in several European WtE installations and it is appreciated for its built-in redundancy in terms of emission control (De Greef et al., 2013) and its flexibility that allows different repartitions of abatement demand between the two stages (Dal Pozzo et al., 2016).

As shown in Fig. 1, the present study is focused on the optimisation of the control of the $Ca(OH)_2$ 1st stage of acid gas removal, referred to in the following as dry sorbent injection (DSI) system. As discussed in the following, the optimisation and tuning of the process control of the 1st stage not only improves the performance of the stage, but, stabilising the HCl outlet concentration, it also favours the optimal performance of the 2nd stage.

2.2 Process control

In the test facility, a conventional process control scheme implemented in several similar plants is present. The operation of the two-stage acid gas abatement system is monitored by the continuous acquisition of flue gas composition data at the measurement points PM1, PM2 and EM indicated in Fig. 1. The concentration of the main gas species at the sampling points, including the acid pollutants (HCl, SO_2, HF), is measured by Fourier-Transform infrared (FTIR) spectrometry, in compliance with CEN/TS 17337 (CEN, 2019), while the flue gas flowrate is determined at stack (point EM) by means of S-type Pitot tube velocity measurements.

In both the acid gas abatement stages, the distributed control system (DCS) of the plant controls the solid reactant feed based on the measured inlet and outlet mass flowrates of acid pollutants. A conditional logic selects the reactant feed rate as the maximum of two values, calculated as follows:

i. *Feedforward criterion*. The calculated feed rate is equal to the stoichiometric demand related to the abatement of the inlet mass flowrates of acid pollutants at PM1, increased by a 10% excess.

ii. *Feedback criterion.* The feed rate is calculated according to a Proportional Integral (PI) feedback formula based on the difference between a set-point for the outlet HCl concentration and the value measured at PM2.

160 The settings of the feedback control (proportional gain K_P = 5 and integral gain τ_I = 8 s)
161 provide an aggressive reaction, i.e. strong excess feed rates of reactant are delivered
162 whenever the outlet HCl concentration exceeds the setpoint. Conversely, when the outlet HCl
163 concentration is lower than the setpoint, the feed rate of reactant does not drop as
164 significantly, because the feedforward criterion takes over. Thus, the combination of the
165 feedforward and feedback criteria as detailed above realises an asymmetrical control action,
166 in which the setpoint is actually treated as a threshold. The feedforward PI control works
167 merely as an environmental safeguard, intended to act only if the feedforward is not capable
168 to maintain the outlet below the given threshold. A survey carried out by the authors involving
169 several Italian companies (HERAmbiente, HestAmbiente, IREN, Brianza Energia Ambiente)
170 evidenced that this control strategy is typical of WtE acid gas abatement units, as the
171 objective is to avoid any spike in outlet HCl resulting from a variation in the inlet HCl load
172 coming from waste combustion (Muratori et al., 2020).
173
174 **2.3 Drawbacks of the reference control system**
175 The typical behaviour of the control system described in section 2.2 is shown in Fig. 2. Most
176 of the time the control operates in feedforward mode and the feed rate of solid reactant is
177 proportional to the inlet HCl load. However, when the outlet HCl flowrate exceeds its setpoint,
178 the feedback mode takes over, imposing a relevant excess in feed rate to bring the HCl outlet
179 back under the threshold as soon as possible. This behaviour determines a peak in reactant
180 consumption but generates also unintended instability in the outlet HCl flow rate. As
181 pinpointed by the arrows in Fig. 2, the spike of reactant feed manages to quickly reduce the
182 outlet HCl flow rate, but such a reduction is often followed by a swift rebound of outlet HCl
183 to high values that triggers another activation of the feedback control, resulting in another

spike of reactant feed. Since the layers of solid reactant accumulated over time on the fabric filter are known to play a major role in the overall acid gas removal action (Kim et al., 2017; Wu et al., 2004), the spikes of reactant feed might be detrimental because they induce unstable operation of the filter (Saleem and Krammer, 2012), activating frequent filter cleaning and reducing the residence time of reactant on the filter. The unstable HCl flow rate at the outlet of the 1st stage can in turn disturb the operation of the 2nd stage of acid gas removal.

In general, this control does not include the minimisation of reactant feed as a criterion and does not realise a rational use of reactant.

3 Methodology

3.1 Framework

Fig. 3 summarises the methodology developed to analyse the performance of alternative process control strategies for DSI, aimed at environmental and economic optimisation. The core element of the methodology is the development of a process simulation that allows exploring alternative control settings in a virtual console, while reducing the need for full-scale test-runs at the real plant. The process simulation duplicates into a software environment the process units and the control system of the actual facility. As sketched in Fig. 3, building the simulation required: i) to reproduce the HCl removal process with a process model; and ii) to simulate the control structure of the DSI unit. The first task required the identification of an appropriate mathematical model for the description of the reaction process (see section 3.2) and its training and validation on plant data collected from test-runs

(see section 3.3). The second task was performed replicating the control architecture of the plant, briefly outlined in section 2.2, with a Simulink block diagram (see section 3.4).

The reliability of the simulation is validated considering the operating process control set-up in the real plant and comparing the outputs of the simulation with those recorded in the plant during normal operation, using the actual data as the input for the simulation. Once validated, the simulation can be used to screen and tune alternative control strategies, eventually leading to a new tuned control strategy that may be tested in the real plant, as in the test case that will be introduced in section 4.

Besides conventional indicators of process control performance, specific environmental and economic indicators (section 3.5) were defined to allow a comprehensive assessment of the performance of the alternative control strategies.

3.2 Selection of data-driven process model and input variables

As mentioned above, a mathematical model is required to reproduce the process dynamics in the simulation. The process model needs to predict how the instantaneous HCl removal efficiency varies depending on the inlet HCl concentration and the feed of solid reactant. Given the intrinsic unsteady nature of the process, this task can be addressed only with a dynamic model capable of handling the rapidly changing operating conditions (e.g. variability of HCl concentration due to variability of waste composition). Existing simplified stationary models of acid gas removal that are typically applied for process optimisation studies (Harriott, 1990; Dal Pozzo et al., 2016) are clearly not apt for this task. On the other hand, phenomenological models (Antonioni et al., 2016; Foo et al., 2017; Montagnaro et al., 2016) that describe rigorously the kinetic and mass transfer phenomena involved in the gas-solid reaction process were typically derived from laboratory-scale data and are not suitable to

simulate full-scale systems, as stated by Gutiérrez Ortiz and Ollero (2008) and Gassner et al. (2014).

Therefore, a data-driven approach was chosen. A system identification procedure was performed to estimate the structure and the parameters of the model from observed input-output plant data (Ljung, 2010). A simple input-output polynomial model, *i.e.* the linear auto-regressive exogenous (ARX) model, was selected as base for the system identification. ARX models have already demonstrated to be reliable tools in emission control problems, e.g. in the prediction of NO_X (Smrekar et al., 2013) or SO_X (Choi et al., 2002) emissions from coal-fired boilers. They are appreciated for their transparency and ease of interpretation (Akinola et al., 2019). The general form of an ARX model is the following:

$$y(t) = a_1 y(t-1) + \cdots + a_{n_a} y(t-n_a) + \sum_i \left[b_{1,i} u_i(t-n_k) + \cdots + b_{n_{b,i}} u_i\left(t - n_{k,i} - n_{b,i} + 1\right) \right] + e(t) \quad (4)$$

where y is the output variable, u_i are the i input variables considered in the model, and e is the white-noise disturbance value. The values a and b are the model parameters, which can be represented in compact form in the parameter vector θ:

$$\theta = \left[a_1 \cdots a_{n_a}\ b_{1,i} \cdots b_{n_{b,i}}\ \right]' \quad (5)$$

This model structure implies that the output variable y at time t is predicted as a linear combination of past output values (autoregressive part of the model) and current and past values of the input variables (exogenous part of the model). The parameters n_a and $n_{b,i}$ are, respectively, the number of past output samples and the number of past input samples (for each input variable i) considered for the prediction of the current output. The model can also

consider input delay terms $n_{k,i}$, i.e. the number of input samples that occur before the input affects the output (also known as the dead time of the system). The use of past observations in the prediction of the output allows approximating also derivative terms by difference quotients, thus enabling the reproduction of the dynamics of the modelled system. The numbers n_a, $n_{b,i}$ and $n_{k,i}$ are known as hyperparameters and represent the order of the model, *i.e.* they indicate the number of parameters to optimise in the training of the model.

For the sake of simplicity, a two-input single-output ARX model was chosen for the present study. The modelled output y is the HCl molar flowrate in the flue gas leaving the DSI system. The two input variables u_i are the inlet HCl molar flowrate and the molar flowrate of $Ca(OH)_2$ fed to the DSI system.

In general, other variables might also affect the HCl removal process. The second most abundant acid compound in WtE flue gases, SO_2, can consume a fraction of the reactant feed (Zhang et al., 2019). Fluctuations in the flue gas flowrate can influence reactant residence time (Hunt and Sewell, 2015). Variations in the operating temperature of the HCl removal stage, e.g. caused by fouling in the heat recovery section upstream, can alter the gas-solid reaction kinetics (Dal Pozzo et al., 2018c). However, variations of temperature and flue gas flowrate are typically limited (see Fig. 2d and 2e) and, in the WtE plant under study, the inlet SO2 concentration was a couple of orders of magnitude lower than that of HCl. Therefore, these variables were excluded in the formulation of the model.

3.3 Calibration of the model

As a data-driven model, the ARX structure requires a specific calibration on data from the actual DSI system modelled. Informative data can be obtained by open-loop tests, in which

the control of the system is deactivated and process performance is assessed by varying manually the feed rate of reactant while recording inlet and outlet HCl concentration.

The dataset Z^N, formed by N consecutive observations of the input and output variables, obtained from the tests has to be divided in: i) a training set Z_{trn}, used for the estimation of the optimal model parameters; and, ii) a cross-validation set Z_{crv}, used for the selection of the optimal order of the model.

A further validation data set, Z_{val}, obtained collecting operating data from the normal, closed-loop operation of the DSI system can be used for the assessment of the performance of the trained model.

Denoting as $\hat{y}(t|\theta)$ the output prediction of the model, least-square method is used to estimate the parameter vector θ^* that produces the best fit of the training data Z_{trn}:

$$\theta^* = \arg\min\{V(\theta, Z_{trn})\}, \qquad \text{where } V(\theta, Z_{trn}) = \frac{1}{N_{trn}} \sum_{t=0}^{N_{trn}-1} \big(y(t) - \hat{y}(t|\theta)\big)^2 \qquad (6)$$

The cross-validation compares the performance of models with different orders, each with its optimal parameter vector θ_i^*, estimated from the training set. The best model is the one for which $V(\theta, Z_{crv})$ is the smallest. This procedure helps selecting a model structure without unnecessary complexity (*i.e.* order), as excessively complex models tend to overfit the training set and perform poorly in the cross-validation set. Lastly, the model with order and parameters optimised for the Z_{trn} and Z_{crv} sets can be tested on the validation set Z_{val} and the procedure can go on iteratively until a given threshold of performance is fulfilled.

3.4 Virtual console

The process model described in section 3.2 was integrated into a simulation environment, where also the control loop and the other components of the DSI system were cloned as in

300 the real plant. The virtual console simulating the operation of the real DSI system consists of
301 four blocks, as shown in Figure 4.
302 The block "*Data import*" defines the inlet conditions of the simulation (inlet HCl concentration
303 and flue gas flowrate). These may be either actual plant data, collected at the measurement
304 point PM1 (see Fig. 1), or artificial data, created to test the system performance under specific
305 strain.
306 The input data of the "*Data Import*" block are then transferred to the *"DTS"* and *"DCS"* blocks.
307 The "*DTS*" block contains the process model described in section 3.2. The "*DCS*" block
308 simulates the control system described in section 2.2. Specifically, given as input signals the
309 HCl load at the inlet of the DTS (provided by the "*Data Import*" block) and the HCl load at the
310 outlet of the dry treatment system (modelled by the "*DTS*" block), this block evaluates with a
311 clock time of 1 s the command input for the actuator that regulates the feed rate of $Ca(OH)_2$.
312 The "*Actuator*" block simulates the operation of the screw feeder installed in the real plant.
313 The virtual actuator receives a percentage command of rotational speed calculated by the
314 "*DCS*" block and transforms it into a molar feed rate of solid reactant to the "*DTS*" block,
315 following a linear relationship between percentage command and feed rate that is
316 characteristic of the real feeder. The response of the actuator was modelled as a first order
317 transfer function:
318
319 $$G(s) = \frac{R}{T_m \cdot s + 1} \quad (7)$$
320
321 where T_m is the actuation time of the screw feeder and R is the command to feed rate ratio.

322 This console allows the comparative testing of the behaviour of the DSI system under the
323 default control (section 2.2) or an alternative control, as discussed in the test case described
324 in section 4.
325
326 **3.5 Performance indicators selected to test alternative control strategies**
327 Both conventional indicators for process control performance and specific indicators
328 capturing the environmental and economic performance of the process were defined to allow
329 a comparison of alternative control strategies. The indicators are reported in Table 1
330 alongside their values obtained for the test case that will be introduced in section 4.
331 With respect to conventional process control indicators, these address the stability of the
332 output variables. The *instability of reactant injection*, expressed as the ratio of the CV of
333 reactant injection to the CV of inlet HCl mass flow, measures the time variability of the feed
334 rate of reactant imposed by the control system. All things equal, a control demanding less
335 variable feed rates is preferred as it induces less mechanical stress on the feeding system. The
336 *instability of HCl outlet*, expressed as the ratio of the CV of outlet HCl mass flow to the CV of
337 inlet HCl mass flow, measures the variability of the HCl mass flow at the outlet of the DSI
338 system.
339 Environmental indicators trace the material streams responsible for the indirect
340 environmental burdens of HCl removal: the *specific consumption of reactant*, expressed as
341 mass of reactant injected per mass of removed HCl, and the *specific generation of residues*,
342 expressed as mass of process residues generated per mass of removed HCl. These indicators
343 were monitored both for the Ca-based 1st stage and the bicarbonate-fed 2nd stage of HCl
344 removal, as the stabilisation of control in the 1st stage (object of the study) can also result in
345 a more stable operation for the 2nd stage. Therefore, an indicator of *overall generation of*

346 *residues*, encompassing both treatment stages, was also considered to have a complete
347 picture of the environmental benefit of control optimisation.
348 Lastly, an indicator addressing *overall operating costs* was also estimated, by translating the
349 streams of reactants and residues in operating costs considering their unit costs (see Table
350 S1).
351

352 # 4 Test Case

353
354 ## 4.1 Definition of the test case

355 The test facility described in section 2.1 was used to define a test case for the application of
356 the methodology outlined in section 3. An open-loop test-run was used for the calibration of
357 the ARX model, while the accuracy of the resulting virtual console in reproducing the system
358 behaviour under its default control was assessed using several datasets available for the
359 normal operation of the DSI system. An example of alternative control was proposed, tuned
360 in the virtual console, then tested by full-scale test-runs on the real plant. The set of indicators
361 defined in section 3.4 was adopted to quantify the improvements in the stability of process
362 control and the economic and environmental performance.
363

364 ## 4.2 Calibration of the model and validation of the simulation for the test case

365 The behaviour of the DSI system of the test facility was studied via step-response tests (Liu
366 and Gao, 2012). Input excitations were applied to the system by varying stepwise the feed
367 rate of $Ca(OH)_2$. The effect on system behaviour was recorded by continuous monitoring (30
368 s resolution time) of the outlet HCl concentration (measurement point PM2 in Fig. 1), while
369 the inlet HCl concentration was also recorded (measurement point PM1 in Fig. 1).

On the basis of the discussion provided in section 3.2, the ARX model was calibrated considering the molar flowrate of inlet HCl (calculated from the measured inlet HCl concentration and inlet flue gas flowrate) and the feed rate of $Ca(OH)_2$ as input variables, while the molar flowrate of outlet HCl (product of the measured outlet HCl concentration and outlet flue gas flowrate) is the modelled output.

The virtual console including the calibrated process model was then validated, comparing its simulated outlet of HCl with the measured values in four datasets of operation of the DSI system under the reference control, provided the same input data (see section 5.1). The simulation error was quantitatively assessed by calculating a cumulative normalised root mean squared error (RMSE):

$$Normalised\ RMSE\ (t) = \frac{\sqrt{\frac{1}{n(t)}\sum_{i=1}^{n(t)}(y_i - \hat{y}_i)^2}}{\frac{\sum_{i=1}^{n(t)} y_i}{n(t)}} \quad (8)$$

where *n(t)* is the number of measurements/model evaluations at a given time.

4.3 Selection and tuning of an alternative control

Once the accuracy of the simulation results was demonstrated, the virtual console was used to test alternative approaches to the control of HCl removal operation. In this test case, the control logic described in section 2.2 (named in the following as "conventional control") was substituted with a simple feedback control (named in the following as "alternative control"). Recalling Fig. 2, the conventional control is built to suppress any overrun of the setpoint of outlet HCl concentration with a spike of $Ca(OH)_2$ feed. The consequences of such approach, as illustrated in section 2.3, are an excess consumption of $Ca(OH)_2$ and unstable inlet conditions for the 2nd HCl removal stage fed with $NaHCO_3$, which, again, lead typically to an

excess consumption of $NaHCO_3$. Conversely, a properly tuned control in purely feedback action could limit the variability of both reactant feed and outlet HCl concentration.

The proposed feedback control is a simple proportional integral (PI) control. As the HCl inlet concentration signal is by nature highly variable and vulnerable to noise contamination (Coleman et al., 2019), the introduction of a derivative (D) control term was avoided, as it could generate system instability (Ting et al., 2008).

Hence, in the simulation the two parameters of the feedback control, K_P gain and τ_I integral time, were tuned. The values of the optimised parameters were K_P = 2 and τ_I = 345 s.

4.4 Performance assessment of the new control at the real plant

Eventually, a comparative assessment of the performance of the conventional and alternative control was carried out at the test facility. The alternative control was easily implemented, by deactivating the feedforward control and updating the feedback settings to the tuned parameters.

The test consisted in comparing a period of DSI process operation with the alternative control with a period of operation with the conventional control. The HCl load released by waste combustion can vary widely over time, and any control logic would manage better a low and uniform inlet mass flow of HCl, rather than a high and fluctuating one. Thus, to ensure a proper comparison, a period of operation experiencing an almost equal inlet mass flow of HCl to that present during the test of the alternative control was selected as representative of the conventional control performance.

As a measure of variability of inlet HCl load, the coefficient of variation (CV) of the HCl mass flow during the test period was estimated:

$$CV = \frac{\sigma}{\mu} \quad (9)$$

where σ and μ are respectively the standard deviation and the mean of the measurements of inlet HCl mass flow during the period of study. It was also ensured that the two periods of DSI operation used for the comparison exhibited a similar CV of HCl mass flow, as it will be discussed in section 5.3. The HCl removal efficiency *X* was also calculated as follows:

$$X = \frac{\dot{m}_{HCl,in} - \dot{m}_{HCl,out}}{\dot{m}_{HCl,in}} \quad (10)$$

The comparison among the performance of the alternative control strategies was carried out calculating the indicators discussed in section 3.5.

5 Results and Discussion

5.1 Results of the validation of the simulation

Figure 5 reports the performance of the virtual console in simulating the behaviour of the conventional process control of the DSI system on a sample dataset (other samples are shown in Figures S1-S3 in the Supporting Information, SI). The percentage command to reactant feed given by the real system and by the simulation are compared in Fig. 5a. Figure 5b compares the measured and the simulated outlet HCl mass flow. The yellow curve represents the set value of outlet HCl mass flow, which is a fluctuating value as it is defined as the product of the fixed setpoint of outlet HCl concentration (see e.g. Fig. 2b) and the variable value of the flue gas flowrate (see e.g. Fig. 2d). Again, it can be noticed that the conventional control treats the set value more like a threshold than a setpoint, as discussed in section 2.3. Figure 5c plots the cumulative average error of the simulation, represented as a normalised RMSE (introduced in section 4.2). The error increases over time, indicating a loss of performance of the process

model nested in the simulation, that is typical of error accumulation in models of autoregressive nature (Bazghaleh et al., 2013; Nelles, 2020). As evidenced also by the figures in the SI, the error grows faster when outlet HCl fluctuates widely, while it remains almost unchanged and may even decrease during periods of stable operation. It is clear that a simple ARX model, linear by nature, falls short of achieving an accurate instantaneous prediction of HCl outlet, which is the result of a complex and non-linear process involving gas-solid reactions both in duct and on filter bags. Nonetheless, the simulation captures the average system behaviour with acceptable resolution for the objective of the study.

5.2 Results of the virtual testing of the alternative control

The simulation was used for the tuning and for the virtual testing of the alternative PI control. The tuning of the alternative control by the methodology outlined in section 4.3 provided the following value for the control parameters: proportional gain K_P = 2 and integral time τ_I of 345 s. It should be recalled that the PI settings of the feedback component of the conventional control (see section 2.2) are K_P = 5 and τ_I = 8 s. The alternative control is less aggressive, with a reduced proportional action and a significantly higher integral time, which lowers the sensitivity of the control action to temporary deviations of the inlet HCl load. Figure 6a illustrates the different behaviour of the alternative control strategy compared to the conventional process control, on a data sample of 100 min. The simulation of the alternative control was started during a significant deviation of the measured HCl outlet concentration from the set-point value to emphasise the different mode of operation of the two control strategies. The feed rate variations imposed by the alternative control strategy are markedly smoother than those of the conventional control. The proposed strategy accepts momentary upticks in the HCl outlet concentration, whereas the action of the original control results in

463 spikes of reactant feed. Conversely, the alternative control strategy imposes a slightly higher
464 feed rate than the original control during periods in which the latter operates in the
465 feedforward mode. These opposite behaviours are evident from the plot of cumulated
466 reactant consumption reported in Fig. 6c. Given that the variability of the reactant feed rate
467 has been highlighted in section 2.3 as one of the main causes of inefficient reactant
468 exploitation in the DTS, the alternative control strategy appears well suited to rationalise the
469 use of the reactant, thus minimising the resulting generation of process residues.
470
471 **5.3 Results of the field test of the alternative control**
472 The alternative PI control was implemented in the DCS of the test facility. As outlined in
473 section 4.4, a test run of the new control was carried out and the resulting operational data
474 were compared with a previous period under the conventional process control configuration.
475 The equivalence of action between the two controls was guaranteed by selecting the average
476 value of outlet HCl concentration in the previous day under the conventional control as the
477 setpoint for the test of the alternative control (see Fig. 7b).
478 Two 5-hour data samples with similar inlet flue gas conditions were selected for the
479 comparative assessment. The two time series are shown in Fig. 7a, where it is possible to
480 compare qualitatively the behaviour of the two control strategies, i.e. the feed rate of
481 reactant and the outlet HCl flowrate, depending on the inlet HCl flowrate. The relative
482 performance of the two controls was tracked via the indicators introduced in section 3.5.
483 Table 1 provides the list of the indicators used and the specific values obtained, while Figure
484 7c shows a radar plot comparing the normalised values of the performance indicators of the
485 alternative control to the reference one. Internal normalisation was used to obtain the values
486 shown in the figure. Given the low inlet SO_2 concentrations measured at the plant (in the

range 10 – 30 mg/Nm^3) and the relatively low reactivity compared to HCl, the effect of SO_2 on system performance is negligible and not discussed in the analysis.

First of all, the two 5-hour data samples present highly comparable inlet HCl loads, hence the two controls are tested in a situation of similar stress. As reported in Table 1, the average inlet HCl mass flow rate in the two periods is equal and its CV is 68% higher during the test of the alternative control, i.e. the selection of data samples is slightly biased in favour of the conventional control.

Figure 7 shows that the real behaviour of the proposed PI-only control is in line with what was expected from the virtual simulation (see Fig. 6). The feed rate varies smoothly, with slow corrections in face of any sharp variation in the outlet HCl flow. Conversely, the conventional control reacts aggressively to deviations in the HCl outlet, with the characteristic spikes of reactant feed rate already described in Fig. 2.

When the performance indicators introduced in section 3.5 are considered, the parameter instability of reactant injection captures numerically this difference: while the commanded feed rate of the original control shows a CV that is 4.3 times higher than the CV of the inlet HCl molar flow, the CV of the commanded feed rate of the proposed control is only 1.24 times higher (a 71% reduction, see Table 1).

At the same time, the specific consumption of reactant in the $Ca(OH)_2$-fed treatment stage is 11% lower with the proposed control. This confirms that the lower aggressivity of the new control settings is not detrimental to the HCl removal efficiency of the system. On the contrary, in the test period, the proposed control managed to achieve the desired HCl removal performance with a significantly lower variability of reactant feed rate, which has the further advantage of reducing the mechanical stress to the screw feeder and the reactant transport system.

Another relevant metric is the instability of the outlet HCl flow, defined in section 3.5 as the ratio between the CVs of outlet and inlet HCl molar flow. The proposed PI-only control achieves a 39% reduction in this indicator. This means that the HCl load exiting the $Ca(OH)_2$-fed treatment stage is less variable in time, thus the downstream $NaHCO_3$-fed stage operates on a less variable HCl inlet and is put in less stressful working conditions. As a consequence, the optimisation of the control in the $Ca(OH)_2$ stage generates also a 26% reduction in the specific consumption of reactant in the subsequent $NaHCO_3$ stage (see again Table 1), whose control was not modified.

The overall consequence of the increase in efficiency owing to the new PI-only control is the reduction in the production of the solid process residues of HCl removal via both the gas-solid reactions with $Ca(OH)_2$ and $NaHCO_3$. The new control achieves a 7% and a 22% reduction in the generation of process residues, respectively in the 1st and 2nd treatment stages. The overall effect is a 13% reduction of the amount of process waste generated by the HCl removal operation. A further confirmation of this effect can be observed in figure S4 in the SI, which shows the simulated action of the conventional control system considering the inlet HCl load for the 5-hour dataset collected during the test-run. The figure evidences that the multiple activations of the feedback mode would have caused a higher reactant consumption.

5.4 Discussion

In the light of the indicators in Table 1, the alternative control strategy tuned in the virtual simulation was demonstrated to improve the overall economic and environmental performance of the system. The consumption of reactants and the generation of process residues were lowered in both the treatment stages, by increasing the efficiency of reactant delivery. It was thus demonstrated that the main drawback of dry acid gas removal, i.e. the

required high excess of reactant, can be partially mitigated by introducing specific process control strategies. In particular, for a multistage system as that of the test facility, it is worth highlighting that an intervention limited to the 1st treatment stage can produce benefits also on the 2nd stage, by enabling a more efficient operation thanks to the lowered variability of the inlet HCl.

The alternative control strategy, based on a PI feedback control, however, has clear limitations: even if the simple feedback action reduces the variability of HCl load compared to the conventional control, the instability with respect to a setpoint is still quite high. More advanced control strategies could offer further improvements. Nonetheless, the proposed solution achieved the results in Table 1 with minimal need of full-scale testing and no significant change in the control architecture of the system, demonstrating the ease of implementation of better solid waste and reactant management via control optimisation.

The results obtained show that the procedure developed for the test of alternative control strategies, based on a virtual console, and the metric introduced, based on the performance indicators listed in Table 1, provide an effective approach to allow the improvement of the environmental and economic operational performance of acid gas treatment systems.

6 Conclusions

With increasingly strict limits on the emission of airborne pollutants as HCl, the flue gas treatment sections in WtE installations are experiencing problems of excessive consumption of reactants and related high generation of solid residues destined to landfilling, which lead to non-negligible indirect environmental burdens. By considering a reference state-of-the-art acid gas removal system, the present study demonstrated that a standard process control

approach based exclusively on the suppression of HCl emissions might be a suboptimal solution in terms of economic and environmental performance. A simple methodology based on virtual simulation and limited full-scale test-runs allowed identifying and tuning an alternative control strategy that achieved a reduction in the generation of solid process residues equal to 7% in the optimised $Ca(OH)_2$-fed 1st stage of HCl removal and 13% in the overall two-stage treatment line with respect to the original control configuration, while maintaining the same HCl emission performance at stack.

Despite the relevant advantages in terms of reactant economy, a limitation of the proposed solution is that it only partially alleviates the fluctuations in the HCl concentration at the outlet of the 1st treatment stage, which are intrinsic to the WtE context. More advanced process control strategies, taking into account process disturbances other than inlet pollutant concentration and reactant feed rate, could be the key to develop plant-specific highly performant model-based control schemes. However, the present study evidenced that process control optimisation is a promising area of improvement in the management of WtE flue gas treatment, not only to improve stable operation, but also to increase significantly the economic and environmental performance of DSI processes without hindering the compliance to emission limits at stack.

References

Akinola, T.E., Oko, E., Gu, Y., Wei, H.-L., Wang, M., 2019. Non-linear system identification of solvent-based post-combustion CO2 capture process. Fuel 239, 1213-1223.

Antonioni, G., Dal Pozzo, A., Guglielmi, D., Tugnoli, A., Cozzani, V., 2016. Enhanced modelling of heterogeneous gas-solid reactions in acid gas removal dry processes. *Chem. Eng. Sci.* 148, 140-154.

Ardolino, F., Boccia, C., Arena, U., 2020. Environmental performances of a modern waste-to-energy unit in the light of the 2019 BREF document. Waste Manage. 104, 94-103.

Arena, U., 2015. From waste-to-energy to waste-to-resources: The new role of thermal treatments of solid waste in the Recycling Society. Waste Manage. 37, 1-2.

Bagheri, M., Esfilar, R., Golchi, M.S., Kennedy, C.A., 2020. Towards a circular economy: A comprehensive study of higher heat values and emission potential of various municipal solid wastes. Waste Manage. 101, 210-221.

Bal, M., Reddy, T.T., Meikap, B.C., 2019. Removal of HCl gas from off gases using self-priming venturi scrubber. J. Haz. Mat. 364, 406-418.

Bazghaleh, M., Mohammadzaheri, M., Grainger, S., Cazzolato, B., Lu, T.-F., 2013. A new hybrid method for sensorless control of piezoelectric actuators. Sensors and Actuators A: Physical 194, 25-30.

Beylot, A., Hochar, A., Michel, P., Descat, M., Ménard, Y., Villeneuve, J., 2018. Municipal Solid Waste Incineration in France: An Overview of Air Pollution Control Techniques, Emissions, and Energy Efficiency. J. Ind. Ecol. 22, 1016-1026.

Bogush, A., Stegemann, J.A., Wood, I., Roy, A., 2015. Element composition and mineralogical characterisation of air pollution control residue from UK energy-from-waste facilities. Waste Manage. 36, 119-129.

CEN, 2019. CEN/TS 17337:2019 – Stationary source emissions - Determination of mass concentration of multiple gaseous species - Fourier transform infrared spectroscopy. European Committee for Standardization, Bruxelles, Belgium.

Choi, S., Yoo, C., Lee, I.-B., 2002. SOx monitoring and neural net classification in the power plant. J. Environ. Eng. 128, 911-918.

Cignitti, S., Mansouri, S.S., Sales-Cruz, M., Jensen, F., Huusom, J.K., 2016. Dynamic Modeling and Analysis of an Industrial Gas Suspension Absorber for Flue Gas Desulfurization. Emiss. Control Sci. Technol. 2, 20-32.

Coleman, M.D., Ellison, M., Robinson, R.A., Gardiner, T.D., Smith, T.O.M., 2019. Uncertainty requirements of the European Union's Industrial Emissions Directive for monitoring sulfur dioxide emissions: Implications from a blind comparison of sulfate measurements by accredited laboratories. J. Air Waste Manage. Assoc. 69, 1070-1078.

Dal Pozzo, A., Moricone, R., Tugnoli, A., Cozzani, V., 2019. Experimental Investigation of the Reactivity of Sodium Bicarbonate toward Hydrogen Chloride and Sulfur Dioxide at Low Temperatures. *Ind. Eng. Chem. Res.* 58, 6316-6324.

615 Dal Pozzo, A., Lazazzara, L., Antonioni, G., Cozzani, V., 2020. Techno-economic
616 performance of HCl and SO2 removal in waste-to-energy plants by furnace direct sorbent
617 injection. *J. Haz. Mat.* 394, 122518.

618 Dal Pozzo, A., Guglielmi, D., Antonioni, G., Tugnoli, A., 2018a. Environmental and
619 economic performance assessment of alternative acid gas removal technologies for
620 waste-to-energy plants. *Sust. Prod. Consumption* 16, 202-215.

621 Dal Pozzo, A., Armutlulu, A., Rekhtina, M., Müller, C.R., Cozzani, V. 2018b. CO2 Uptake
622 Potential of Ca-Based Air Pollution Control Residues over Repeated Carbonation-
623 Calcination Cycles. *Energy Fuels* 32, 5386-5395.

624 Dal Pozzo, A., Giannella, M., Antonioni, G., Cozzani, V., 2018c. Optimization of the
625 economic and environmental profile of HCl removal in a municipal solid waste incinerator
626 through historical data analysis. *Chem. Eng. Trans.* 67, 463-468.

627 Dal Pozzo, A., Guglielmi, D., Antonioni, G., Tugnoli, A., 2017. Sustainability analysis of dry
628 treatment technologies for acid gas removal in waste-to-energy plants. *J. Clean. Prod.* 162,
629 1061-1074.

630 Dal Pozzo, A., Antonioni, G., Guglielmi, D., Stramigioli, C., Cozzani, V., 2016. Comparison
631 of alternative flue gas dry treatment technologies in waste-to-energy processes. *Waste*
632 *Manage.* 51, 81-90.

633 Damgaard, A., Riber, C., Fruergaard, T., Hulgaard, T., Christensen, T.H., 2010. Life-cycle-
634 assessment of the historical development of air pollution control and energy recovery in
635 waste incineration. *Waste Manage.* 30, 1244-1250.

636 De Greef, J., Villani, K., Goethals, J., Van Belle, H., Van Caneghem, J., Vandecasteele, C.,
637 2013. Optimising energy recovery and use of chemicals, resources and materials in
638 modern waste-to-energy plants. Waste Manage. 33, 2416-2424.

639 Dong, J., Jeswani, H.K., Nzihou, A., Azapagic, A., 2020. The environmental cost of
640 recovering energy from municipal solid waste. Appl. Energy 267, 114792.

641 Ephraim, A., Ngo, L.D., Pham Minh, D., Lebonnois, D., Peregrina, C., Sharrock, P., Nzihou,
642 A., 2019. Valorization of Waste-Derived Inorganic Sorbents for the Removal of HCl in
643 Syngas. Waste Biomass Valorization 10, 3435-3446.

644 Foo, R., Berger, R., Heiszwolf, J.J., 2016. Reaction Kinetic Modeling of DSI for MATS
645 Compliance. In: Proceedings of the Power Plant Pollutant Control and Carbon
646 Management “MEGA” Symposium, Baltimore, MD, USA, 16–19 August 2016

647 Gassner, M., Nilsson, J., Nilsson, E., Palmé, T., Züfle, H., Bernero, S., 2014. A data-driven
648 approach for analysing the operational behaviour and performance of an industrial flue
649 gas desulphurisation process. Computer Aided Chem. Eng. 33, 661-666.

650 Gerassimidou, S., Velis, C.A., Williams, P.T., Castaldi, M.J., Black, L., Komilis, D., 2020.
651 Chlorine in waste-derived solid recovered fuel (SRF), co-combusted in cement kilns: A
652 systematic review of sources, reactions, fate and implications. Critical Reviews in
653 Environmental Science and Technology, in press.

654 Goodall, P.; Sharpe, R.; West, A., 2019. A data-driven simulation to support
655 remanufacturing operations. Computers in Industry 105, 48-60.

656 Guo, Y., Xu, Z., Zheng, C., Shu, J., Dong, H., Zhang, Y., Weng, W., Gao, X., 2019. Modeling
657 and optimization of wet flue gas desulfurization system based on a hybrid modeling
658 method. J. Air Waste Manage. Assoc. 69, 565-575.

659 Gutiérrez Ortiz, F.J., Ollero, P., 2008. A realistic approach to modeling an in-duct
660 desulfurization process based on an experimental pilot plant study. *Chem. Eng. J.* 141,
661 141-150.

662 Harriott, P., 1990. A Simple Model for SO_2 Removal in the Duct Injection Process. J. Air
663 Waste Manage. Assoc. 40, 998-1003.

664 Hartman, M., Svoboda, K., Pohorely, M., Syc, M., 2013. Thermal Decomposition of Sodium
665 Hydrogen Carbonate and Textural Features of Its Calcines. Ind. Eng. Chem. Res. 52, 10619-
666 10626.

667 Hunt, G., Sewell, M., 2015. Utilizing Dry Sorbent Injection Technology to Improve Acid Gas
668 Control. In: 34th International Conference on Thermal Treatment Technologies &
669 Hazardous Waste Combustors, Houston, TX, USA, 20-22 October 2015

670 Iizuka, A., Morishita, Y., Shibata, E., Takatoh, C., Cho, H., 2020. Basic Study of the Reaction
671 of Calcium Hydroxide with Hydrogen Chloride Using Single Crystals. *Ind. Eng. Chem. Res.*
672 59, 9699-9704.

673 Kameda, T., Tochinai, M., Kumagai, S., Yoshioka, T., 2020. Treatment of HCl gas by cyclic
674 use of Mg–Al layered double hydroxide intercalated with CO32-. Atmospheric Pollution
675 Res. 11, 290-295.

676 Kim, K.-D., Jeon, S.-M., Hasolli, N., Lee, K.-S., Lee, J.-R., Han, J.-W., Kim, H.T., Park, Y.-O.,
677 2017. HCl removal characteristics of calcium hydroxide at the dry-type sorbent reaction
678 accelerator using municipal waste incinerator flue gas at a real site. Korean J Chem Eng
679 34, 747-756.

680 Kockmann, N., 2019. Digital methods and tools for chemical equipment and plants.
681 Reaction Chemistry and Engineering 4, 1522-1529.

682 Lausselet, C., Cherubini, F., del Alamo Serrano, G., Becidan, M., Strømman, A.H., 2016.
683 Life-cycle assessment of a Waste-to-Energy plant in central Norway: Current situation and
684 effects of changes in waste fraction composition. Waste Manage. 58, 191-201.

685 Liu, T., Gao, F., 2012. Step Response Identification of Stable Processes. In: Liu, T., Gao, F.,
686 Industrial Process Identification and Control Design, Springer-Verlag London, London, UK.

687 Liu, S., Sun, L., Zhu, S., (...), Chen, X., Zhong, W., 2020. Operation strategy optimization of
688 desulfurization system based on data mining. Appl. Mathematical Modelling 81, 144-158.

689 Ljung, L., 2010. Perspectives on system identification. Annual Reviews in Control 34, 1-12.

690 Margallo, M., Taddei, M.B.M., Hernández-Pellón, A., Aldaco, R., Irabien, A., 2015.
691 Environmental sustainability assessment of the management of municipal solid waste
692 incineration residues: A review of the current situation. Clean Technol. Environ. Policy 17,
693 1333-1353.

694 Montagnaro, F., Balsamo, M., Salatino, P., 2016. A single particle model of lime sulphation
695 with a fractal formulation of product layer diffusion. Chem. Eng. Sci. 156, 115-120.

Muratori, G., Dal Pozzo, A., Antonioni, G., Cozzani, V., 2020. Application of Multivariate Statistical Methods to the Modelling of a Flue Gas Treatment Stage in a Waste-to-energy Plant. *Chem. Eng. Trans.* 82, 397-402.

Nelles, O., 2020. Nonlinear System Identification: From Classical Approaches to Neural Networks, Fuzzy Models, and Gaussian Processes. Springer Nature, Berlin, Germany.

Neuwahl, F., Cusano, G., Gomez Benavides, J., Holbrook, S., Roudier, S., 2019. Best Available Techniques (BAT) Reference Document for Waste Incineration. EUR 29971 EN. doi:10.2760/761437

Ouda, O.K.M., Raza, S.A., Nizami, A.S., Rehan, M., Al-Waked, R., Korres, N.E., 2016. Waste to energy potential: A case study of Saudi Arabia. Renewable Sustainable Energy Reviews 61, 328-340.

Peng, H., Ozaki, T., Toyoda, Y., Shioya, H., Nakano, K., Haggan-Ozaki, V., Mori, M., 2004. RBF-ARX model-based nonlinear system modeling and predictive control with application to a NOx decomposition process. Control Engineering Practice 12, 191-203.

Quina, M.J., Bontempi, E., Bogush, A., Schlumberger, S., Weibel, G., Braga, R., Funari, V., Hyks, J., Rasmussen, E., Lederer, J., 2018. Technologies for the management of MSW incineration ashes from gas cleaning: New perspectives on recovery of secondary raw materials and circular economy. Sci. Total Environ. 635, 526-542.

Saleem, M., Krammer, G., 2012. On the Stability of Pulse-Jet Regenerated-Bag Filter Operation. Chemical Engineering and Technology 35, 877-884.

Smrekar, J., Potočnik, P., Senegačnik, A., 2013. Multi-step-ahead prediction of NOx emissions for a coal-based boiler. Appl. Energy 106, 89-99.

Ting, C.-H., Chen, H.-H., Yen, C.-C., 2008. A PID ratio control for removal of HCl/SOx in flue gas from refuse municipal incinerators. Control Engineering Practice 16, 286-293.

Van Caneghem, J., Van Acker, K., De Greef, J., Wauters, G., Vandecasteele, C., 2019. Waste-to-energy is compatible and complementary with recycling in the circular economy. Clean Technol. Environ. Policy, in press.

Vehlow, J., 2015. Air pollution control systems in WtE units: An overview. *Waste Manage.* 37, 58-74.

Wu, C., Kang, S.-J., Keener, T.C., Lee, S.-K., 2004. A model for dry sodium bicarbonate duct injection flue gas desulfurization. Advances in Environmental Research 8, 655-666.

Yang, N., Damgaard, A., Scheutz, C., Shao, L.-M., He, P.-J., 2018. A comparison of chemical MSW compositional data between China and Denmark. J. Environ. Sci. 74, 1-10.

Zhang, H., Yu, S., Shao., L., He, P., 2019. Estimating source strengths of HCl and SO2 emissions in the flue gas from waste incineration. J. Environ. Sci. 75, 370-377.

Figures and Tables

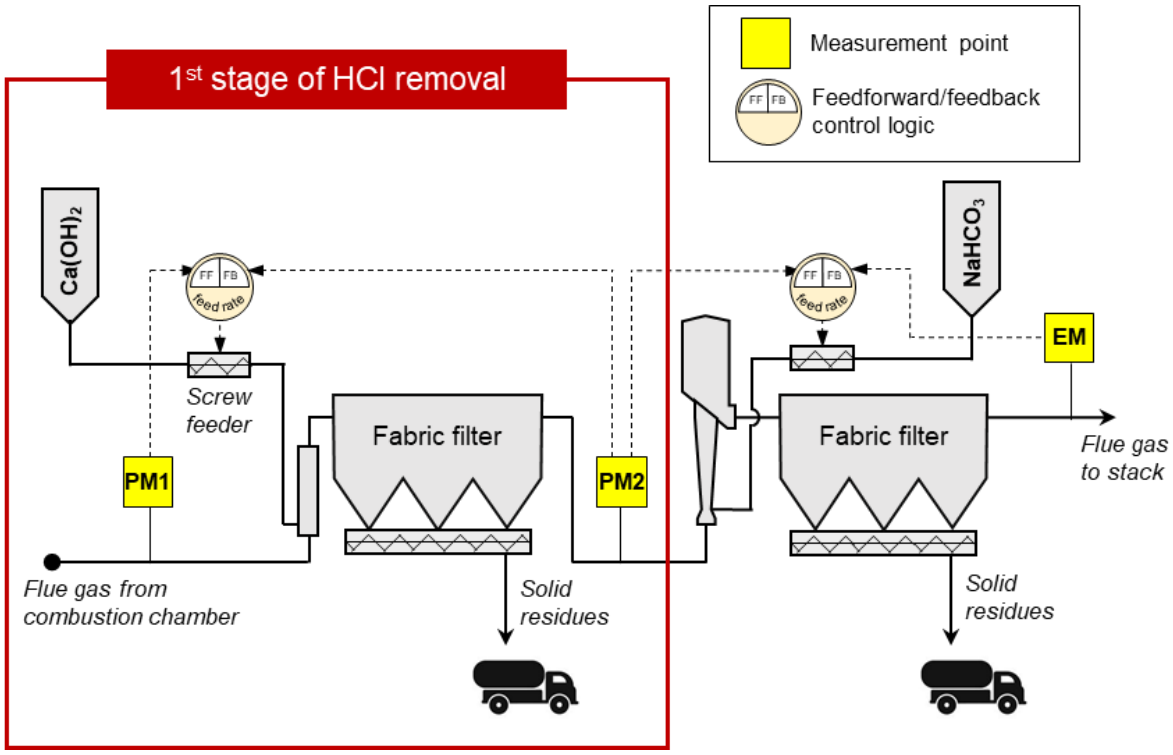

Figure 1. *Scheme of the two-stage acid gas abatement system of the test facility considered, including measurement points of flue gas composition (PM1, PM2 = process measurement, EM = measurement at stack) and control loops for reactant feed rate. Control optimization of 1st stage (red box in the figure) was the object of the study.*

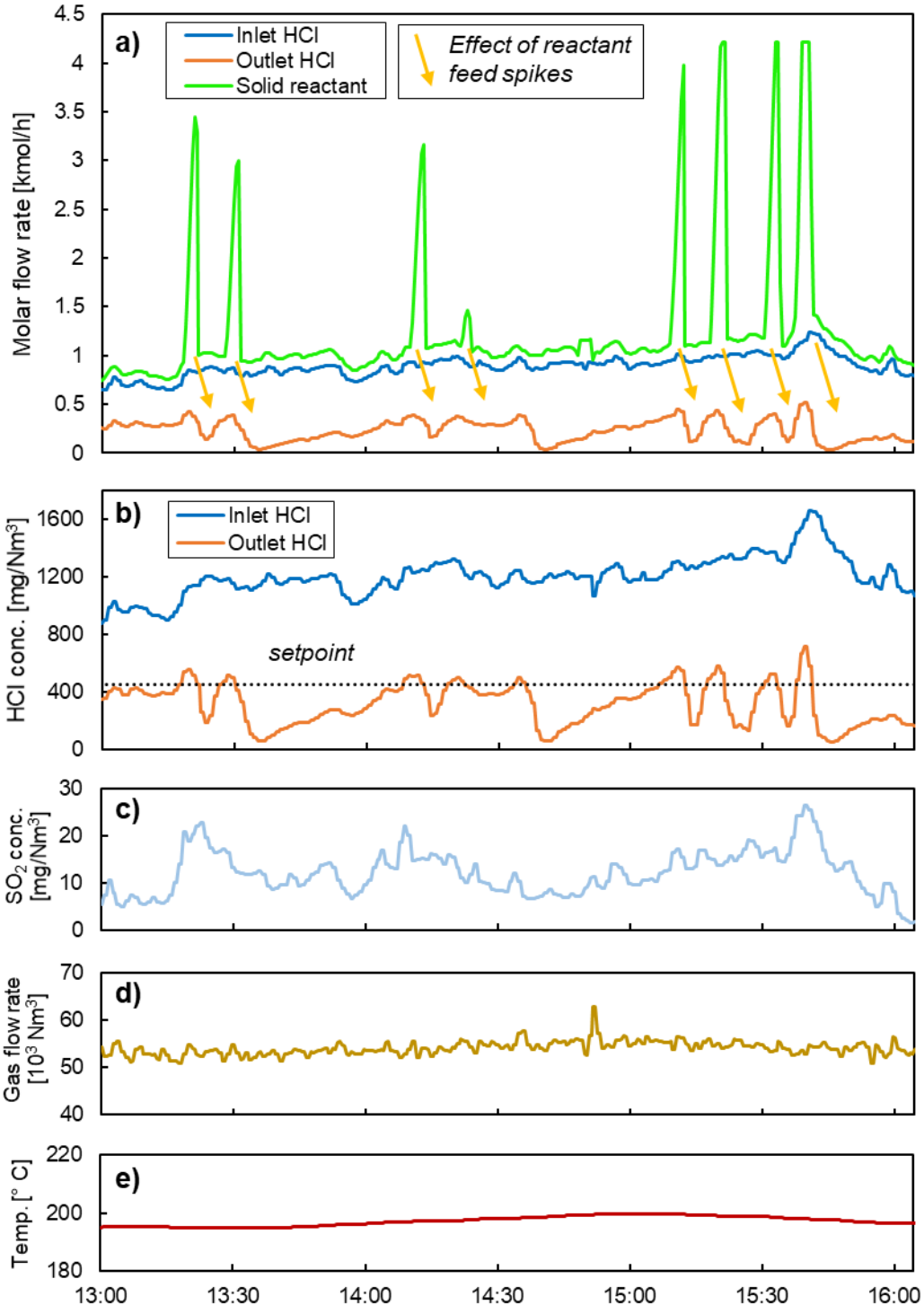

744

745 **Figure 2.** *Data recorded by the distributed control system (DCS) of an Italian WtE facility*
746 *showing: a) the typical trend of inlet and outlet HCl flowrate and solid reactant feed rate*
747 *during normal operation of the 1st stage acid gas removal unit applying the conventional*
748 *process control strategy; b) threshold setpoint with respect to HCl inlet and outlet*
749 *concentrations; c) SO_2 concentration; d) flue gas flowrate; e) operating temperature.*

750

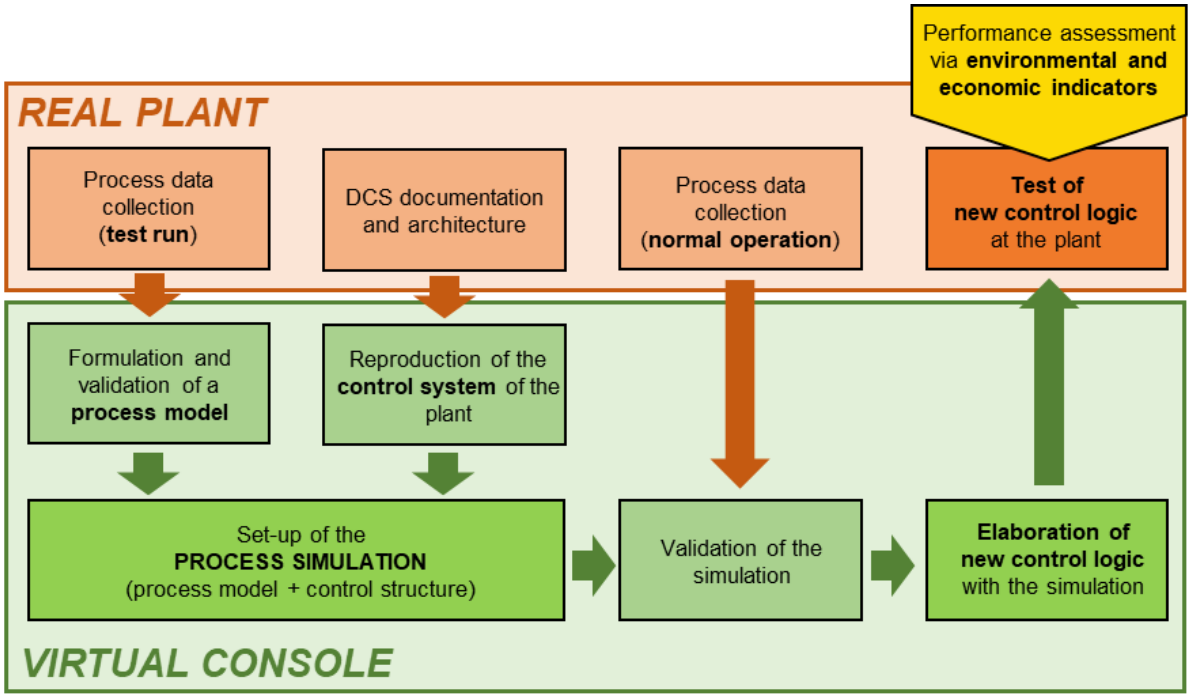

751

752 **Figure 3.** *Methodology developed for testing and tuning of improved process control*

753 *strategies.*

754

755

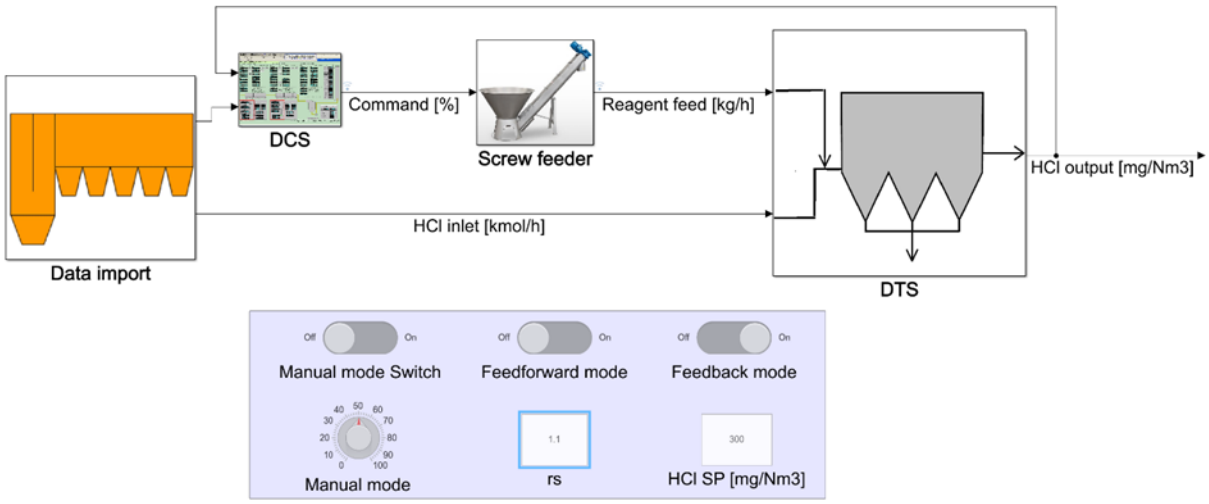

756

757 **Figure 4.** *Virtual console developed to simulate the DSI process (1st stage of the acid gas*

758 *removal system in Fig. 1) using the Simulink® software tool.*

759

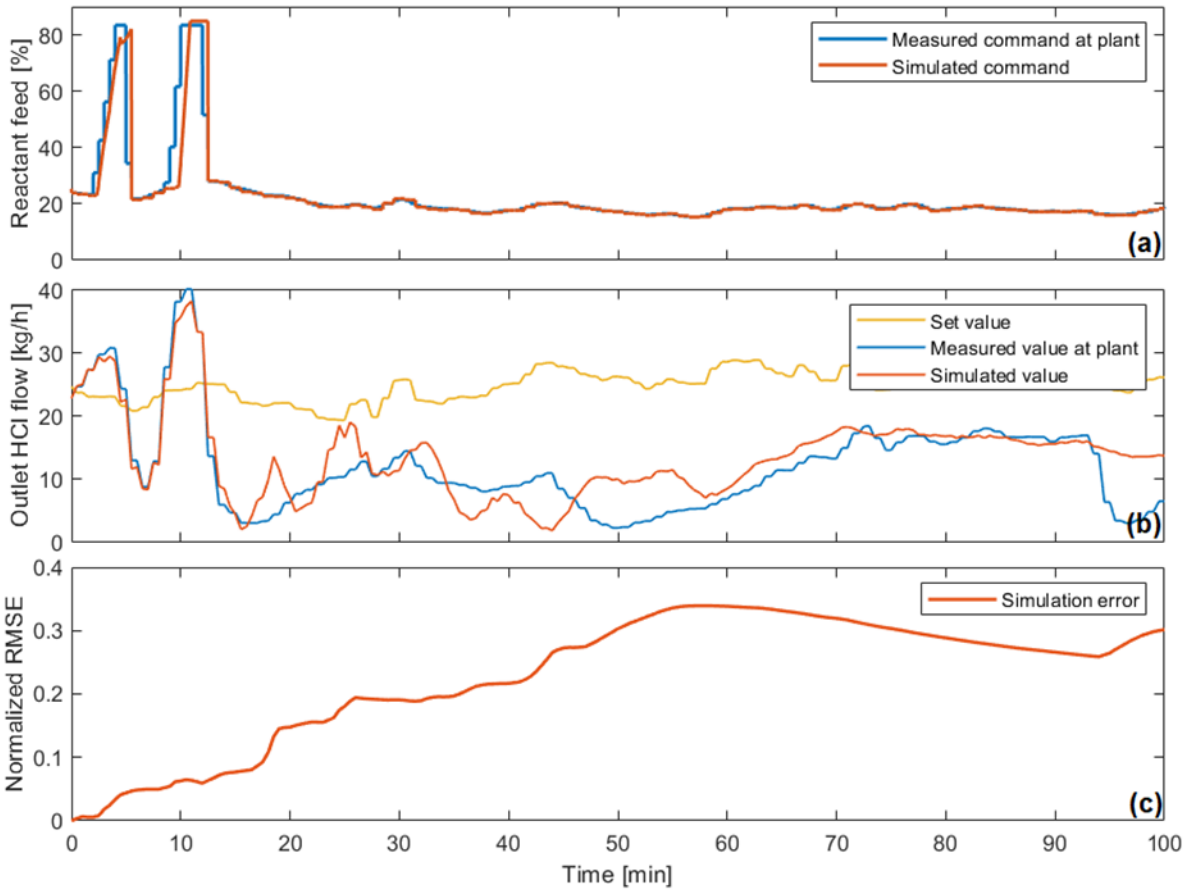

760
761

762 **Figure 5.** *Performance of the virtual console in simulating the behaviour of the conventional*

763 *control of the system: a) measured vs. simulated command of reactant feed, b) measured vs.*

764 *simulated outlet HCl flow rate, compared to the set value of the control, c) cumulative average*

765 *error of the simulation.*

766

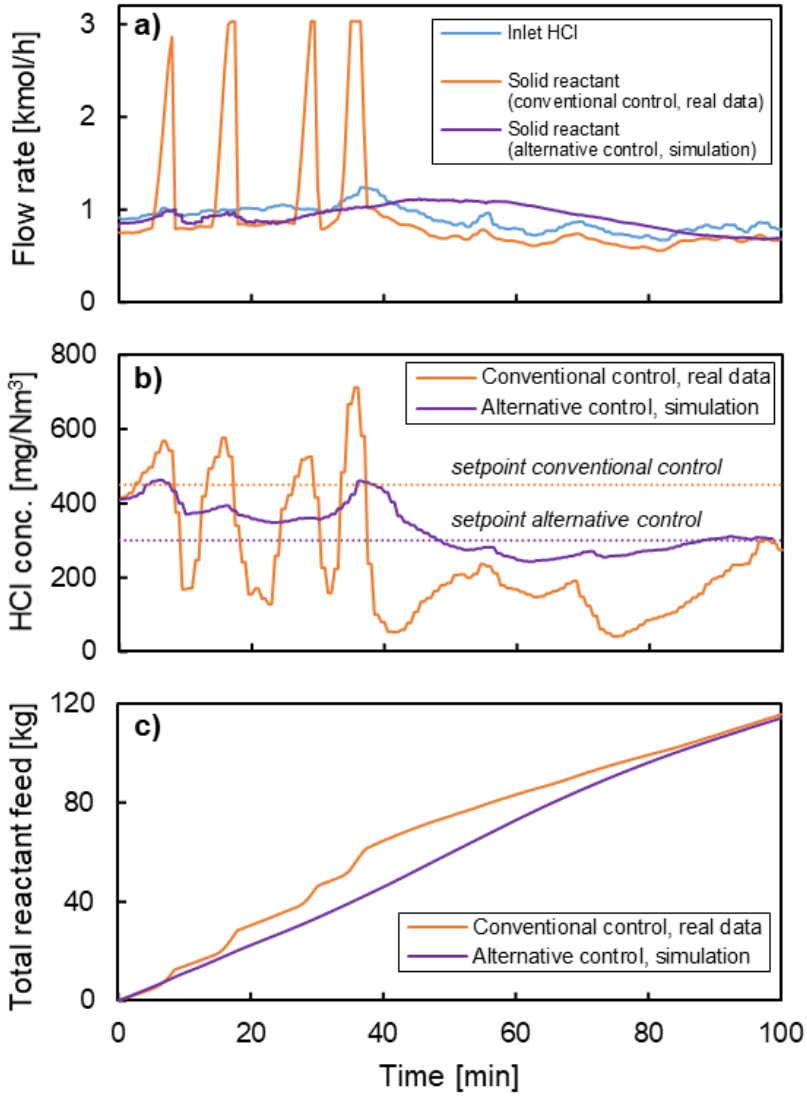

767

768 **Figure 6.** a) *Simulation of the reactant feed rate by the alternative PI control strategy*

769 *compared to the conventional process control on a sample dataset; b) deviation of the outlet*

770 *HCl concentration from the respective setpoints, c) resulting cumulated reactant consumption.*

771

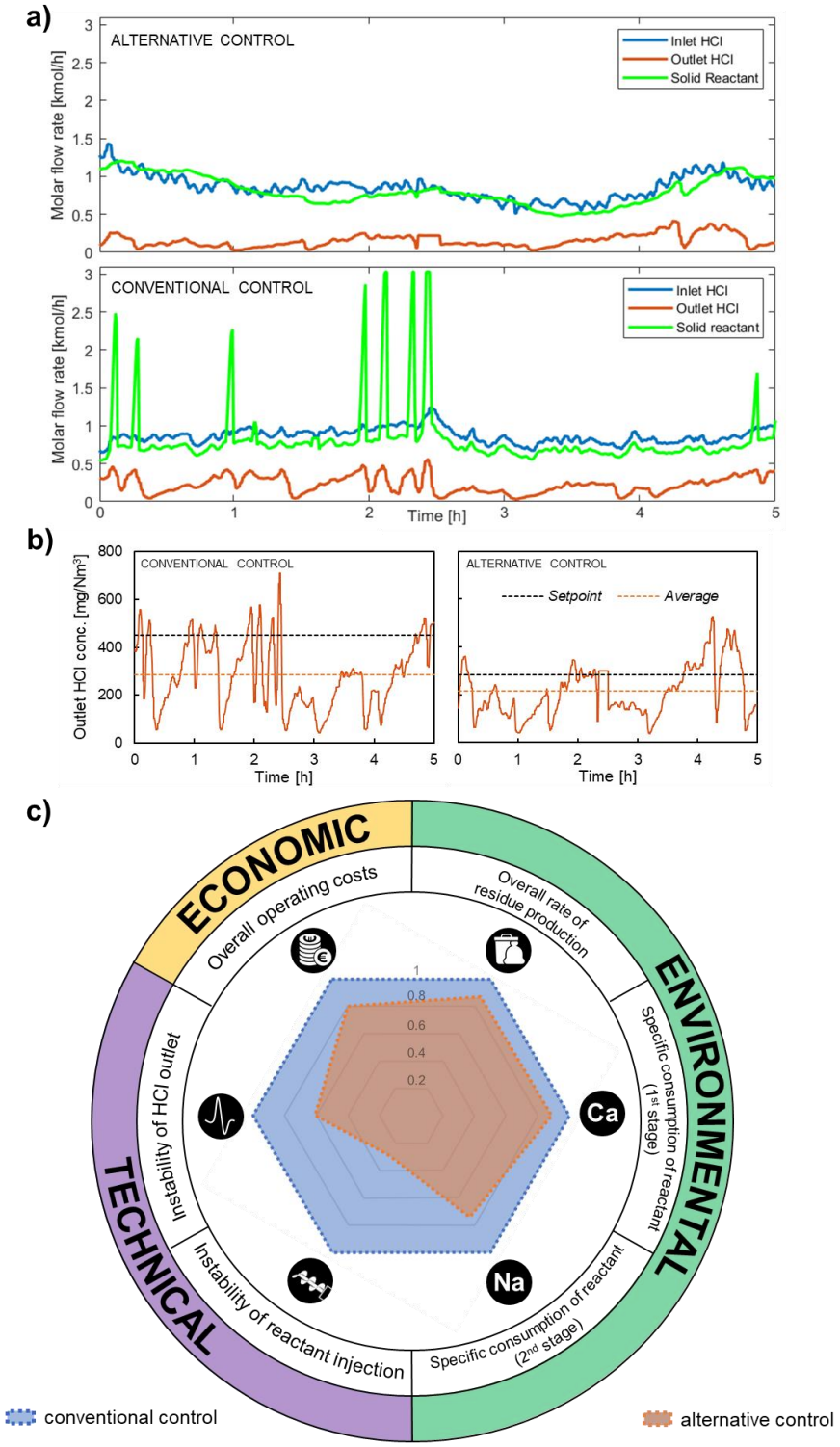

772

773 **Figure 7.** *Results of test-run: a) 5-hour data samples obtained during alternative process*
774 *control and conventional process control operation under a similar HCl input, b) outlet HCl*
775 *concentration in the two 5-hour data samples, c) comparison between the normalised*
776 *performance indicators of the alternative process control strategy to the conventional process*
777 *control.*

778 **Table 1.** *Performance of the alternative control strategy vs. the conventional process control*

779 *monitored according to the performance indicators introduced in section 3.5.*

Parameter or indicator		Test period		Δ
		Conventional control	Alternative control	
Inlet HCl mass flow rate (kg/h)	μ	64.4	64.4	-
	CV	0.12	0.19	+68%
Feed rate of reactant, $Ca(OH)_2$ (kg/h)	μ	61.1	60.0	-2%
	CV	0.49	0.24	-52%
Outlet HCl mass flow rate (kg/h)	μ	17.2	12.5	-27%
	CV	0.51	0.52	+2%
HCl removal efficiency (%)	μ	75.8	82.3	+9%
	CV	11.2	8.5	-24%
Instability of reactant injection (CV of $Ca(OH)_2$ feed rate / CV of inlet HCl)		4.27	1.24	**-71%**
Instability of HCl outlet (CV of outlet HCl / CV of inlet HCl)		4.4	2.7	**-39%**
Specific consumption of reactant (1^{st} stage) (kg of $Ca(OH)_2$ fed / kg of HCl removed)		1.30	1.16	**-11%**
Specific generation of residues (1^{st} stage) (kg of residues / kg of HCl removed)		1.80	1.67	**-7%**
Specific consumption of reactant (2^{nd} stage) (kg of $NaHCO_3$ fed / kg of HCl removed)		3.85	2.86	**-26%**
Specific generation of residues (2^{nd} stage) (kg of residues / kg of HCl removed)		2.55	2.00	**-22%**
Overall rate of residue production (kg of residues / kg of HCl removed)		2.00	1.73	**-13%**
Overall economic performance (€ of operating costs / kg of HCl removed)		1.86	1.48	**-20%**

780

781

Declaration of interests

☒ The authors declare that they have no known competing financial interests or personal relationships that could have appeared to influence the work reported in this paper.

☐The authors declare the following financial interests/personal relationships which may be considered as potential competing interests:

Click here to access/download
Supplementary Material
Suppl Info WM_Control_revFINAL.docx